BRIEF REPORT

Human Mutation

OFFICIAL JOURNAL

HGVS HUMAN GENOME VARIATION SOCIETY

www.hgvs.org

KDM6A Point Mutations Cause Kabuki Syndrome

Noriko Miyake,[1]* Seiji Mizuno,[2] Nobuhiko Okamoto,[3] Hirofumi Ohashi,[4] Masaaki Shiina,[5] Kazuhiro Ogata,[5] Yoshinori Tsurusaki,[1] Mitsuko Nakashima,[1] Hirotomo Saitsu,[1] Norio Niikawa,[6] and Naomichi Matsumoto[1]

[1]Department of Human Genetics, Yokohama City University Graduate School of Medicine, Yokohama, Japan; [2]Department of Pediatrics, Central Hospital, Aichi Human Service Center, Kasugai, Japan; [3]Division of Medical Genetics, Osaka Medical Center and Research Institute for Maternal and Child Health, Izumi, Japan; [4]Division of Medical Genetics, Saitama Children's Medical Center, Iwatsuki, Japan; [5]Department of Biochemistry, Yokohama City University Graduate School of Medicine, Yokohama, Japan; [6]Research Institute of Personalized Health Sciences, Health Science University of Hokkaido, Hokkaido, Japan

Communicated by Garry R. Cutting

Received 7 August 2012; accepted revised manuscript 18 September 2012.
Published online 19 October 2012 in Wiley Online Library (www.wiley.com/humanmutation). DOI: 10.1002/humu.22229

ABSTRACT: Kabuki syndrome (KS) is a rare congenital anomaly syndrome characterized by a unique facial appearance, growth retardation, skeletal abnormalities, and intellectual disability. In 2010, *MLL2* was identified as a causative gene. On the basis of published reports, 55–80% of KS cases can be explained by *MLL2* abnormalities. Recently, de novo deletion of *KDM6A* has been reported in three KS patients, but point mutations of *KDM6A* have never been found. In this study, we investigated *KDM6A* in 32 KS patients without an *MLL2* mutation. We identified two nonsense mutations and one 3-bp deletion of *KDM6A* in three KS cases. This is the first report of *KDM6A* point mutations associated with KS.
Hum Mutat 34:108–110, 2013. © 2012 Wiley Periodicals, Inc.

KEY WORDS: Kabuki syndrome; *KDM6A*; point mutations; chromosome X

Kabuki syndrome (KS; MIM# 147920), first described by Niikawa and Kuroki in 1981, is a rare congenital anomaly syndrome with the characteristic facial features of a long palpebral fissure and eversion of lateral third of the inferior eyelids [Kuroki et al., 1981; Niikawa et al., 1981]. Individuals with KS also show mild to severe intellectual disability, growth retardation, skeletal abnormalities, and a variety of visceral malformations. Although KS is thought to inherit in autosomal dominant fashion, other inheritance patterns have also been considered [Matsumoto and Niikawa, 2003]. In 2010, whole exome sequencing successfully identified loss-of-function mutations in *MLL2* in KS. *MLL2* maps to 12q13.12 and consists of at least 54 coding exons. *MLL2* encodes a histone H3 lysine 4 (H3K4)-specific methyl transferase and plays important roles in the epigenetic control of active chromatin states. On the basis of recent reports of *MLL2* mutations in KS, the mutation detection rate of *MLL2* in KS is 55–80% [Banka et al., 2012]. Among the published mutations, 73.2% (170/232) were truncation type, and pathogenic missense mutations were mainly localized in exon 48 [Banka et al., 2012].

X-linked inheritance has also been implicated in KS. Sex chromosome abnormalities in KS have been reported many times and some of the clinical manifestations are shared with Turner syndrome; patients showing overlapping features, called "Turner–Kabuki" syndrome, have been reported [Bianca et al., 2009; Dennis et al., 1993; Niikawa et al., 1988; Rodriguez et al., 2008; Stankiewicz et al., 2001; Wellesley and Slaney, 1994]. Common structural abnormalities (inversion, translocation, and ring chromosome) involving Xp11 and Yp11 in the pseudoautosomal region were observed in KS, implying the potential involvement of the regions for pathogenesis in KS [Matsumoto and Niikawa, 2003]. In addition, two unrelated KS patients with ring X (p11.2q13) have been reported [McGinniss et al., 1997; Niikawa et al., 1988]. However, an X-linked gene for KS has not been identified until recently. In 2012, complete or partial de novo deletions of *KDM6A* (MIM# 300228) were identified in three patients with KS [Lederer et al., 2012]. *KDM6A* resides at Xp11.3 and encodes the lysine demethylase 6A (KDM6A) demethylating di- and trimethyl-lysine 27 on histone H3 (H3K27) [Lee et al., 2007]. H3K4 methylation by MLL2/3 is linked to the demethylation of H3K27 by KDM6A [Lee et al., 2007]. These authors sequenced *KDM6A* in their series of 22 patients, but found no point mutations [Lederer et al., 2012]. In this study, we investigated *KDM6A* with regard to point mutations in KS after obtaining written informed consents from families of patients. The institutional review board of Yokohama City University School of Medicine approved this study.

To identify *KDM6A* mutations in KS, we examined this gene's 29 coding exons along with its exon–intron boundaries (NM_021140.2) in 32 KS individuals with no *MLL2* mutation, using high-resolution melting analysis combined with direct sequencing. We identified three mutations: c.3717G>A (p.Trp1239*) in patient 1 (male, hemizygous), c.1555C>T (p.Arg519*) in patient 2 (male, hemizygous), and c.3354_3356delTCT (p.Leu1119del) in patient 3 (female, heterozygous) (Fig. 1). Nucleotide numbering reflects cDNA numbering with +1 corresponding to the A of the ATG translation initiation codon in the reference sequence (NM_021140.2), according to journal guidelines (www.hgvs.org/mutnomen). The initiation codon is codon 1. One mutation (c.3354_3356delTCT) occurred de novo; parental samples were unavailable for the other two. Because the two nonsense mutations were outside of the last

Additional Supporting Information may be found in the online version of this article.

*Correspondence to: Noriko Miyake, Department of Human Genetics, Yokohama City University Graduate School of Medicine, 3–9 Fukuura, Kanazawa-ku, Yokohama 236–0004, Japan. E-mail: nmiyake@yokohama-cu.ac.jp or Naomichi Matsumoto, E-mail: naomat@yokohama-cu.ac.jp

Contract grant sponsors: Ministry of Health, Labour, and Welfare (Japan) (to N.Mi., H.S., and N.Ma.); Japan Science and Technology Agency (to N.Ma.); Strategic Research Program for Brain Sciences from the Ministry of Education, Culture, Sports, Science, and Technology of Japan (to N.Ma.); Japan Society for the Promotion of Science (to N.Mi., H.S., and N.Ma.); Strategic Research Promotion of Yokohama City University (to N.Ma.); Takeda Science Foundation (to N.Mi. and N.Ma.).

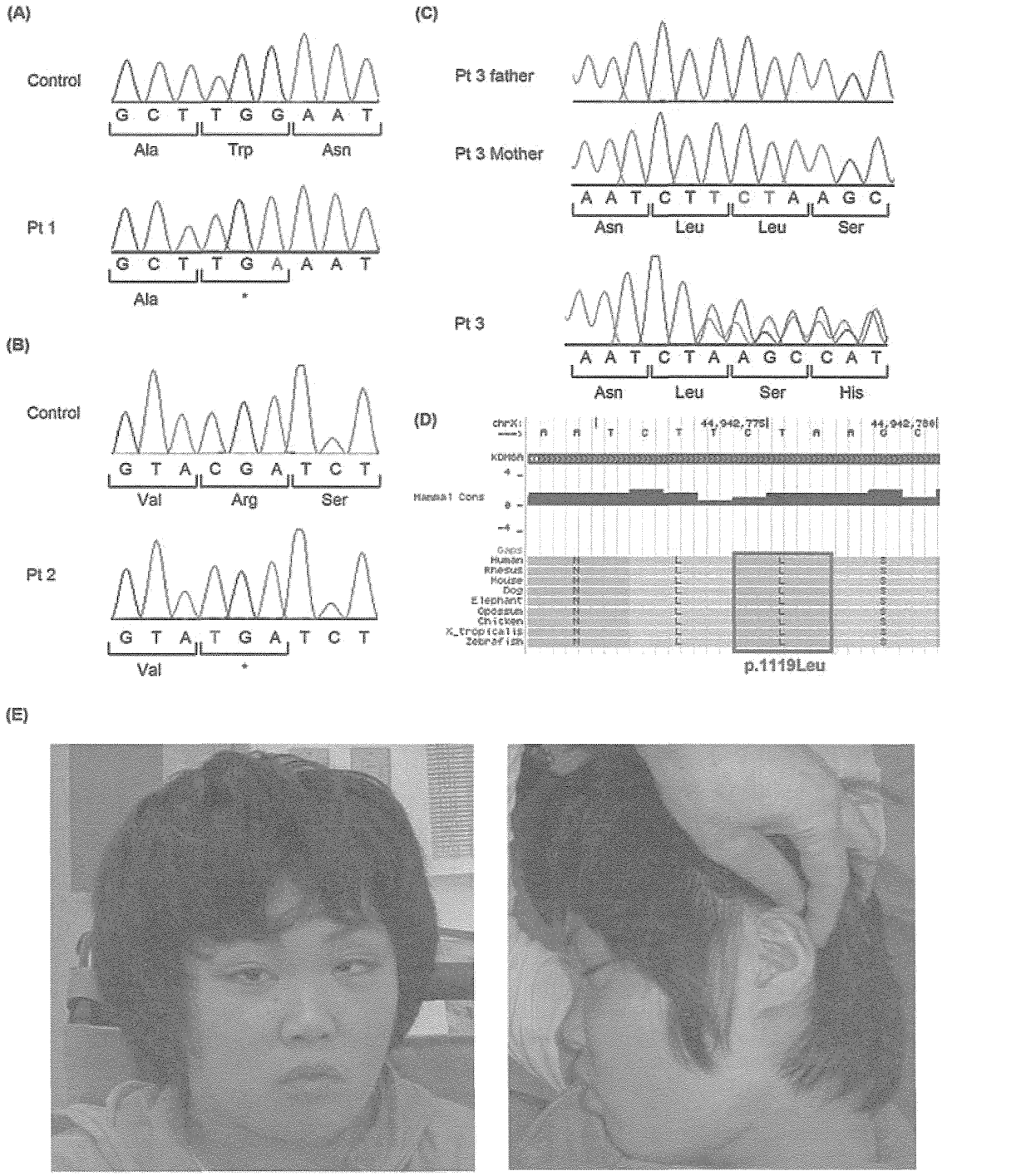

Figure 1. *KDM6A* mutations in three Kabuki syndrome patients. **A–C:** Electropherogram of patient 1: c.3717G>A (p.Trp1239*) (**A**), patient 2: c.1555C>T (p.Arg519*) (**B**), and patient 3: c.3354_3356delTCT (p.Leu1119del) (**C**). Hemizygous changes (**A** and **B**) and a heterozygous change (**C**) can be seen. The altered or deleted nucleotides are written in red. **D:** p. Leu1119 is evolutionarily conserved from zebrafish to human. The position of p.Leu1119 is boxed in red. **E:** Facial photographs of patient 3.

coding exon, and in an exon 55 bp from the 3′ most exon–exon junction, the mutant alleles could be subjected to nonsense-mediated mRNA decay (unfortunately living cells from the patients were unavailable, so we could not test this hypothesis). c.3354_3356delTCT in patient 3 would lead to deletion of one amino acid within the functionally important catalytic Jumonji C (JmjC) domain [Lee et al., 2007]. The amino residue p.Leu1119 is evolutionarily conserved from zebrafish to human (Fig. 1D) and plays an important role in hydrophobic core formation with p.Ile1126 and p.Met1129 to stabilize the JmjC domain [Sengoku and Yokoyama, 2011]. This amino acid deletion may impair helix formation around the mutated residue, resulting in domain destabilization.

Basically, *KDM6A*/*Kdm6a* escapes X-inactivation in humans and mice [Greenfield et al., 1998; Xu et al., 2008]. However, its expression from the inactive X chromosome is lower (15–35%) than that from the active X chromosome in female mice; thus, *Kdm6a* expression

Table 1. Clinical Features of Patients with a *KDM6A* Mutation

	Patient 1	Patient 2	Patient 3
Sex	Male	Male	Female
Mutation	c.3717G>A	c.1555C>T	c.3354_3356delTCT
Protein change	p.Trp1239*	p.Arg519*	p.Leu1119del
De novo status	NA	NA	De novo
Paternal age at birth	34	42	27
Maternal age at birth	33	40	26
Characteristic face	+	+	+
Microcephaly	+	+	–
Long palpebral fissures	+	+	+
Epicanthus	+	–	–
Lower palpebral eversion	+	+	+
Prominent ear	+	+	–
Auricular deformity	+	+	–
Depressed nasal tip	+	+	NA
Short nasal septum	+	+	NA
Abnormal dentition	+	+	–
Hypodontia	+	+	–
High-arched palate	+	+	–
Micrognathia	+	–	–
Short fifth finger	+	–	+
Developmental delay	+ (Severe)	+ (Severe)	+ (Severe)
Intellectual disability	+ (Severe)	+ (Severe)	+ (Severe)
Short stature	+	+	+
Prenatal growth retardation	+ (−1.96 SD)	+	–
Postnatal growth retardation	+	+	+
Cardiovascular abnormality	+	–	–
Joint laxity	+	+	–
Recurrent otitis media	+	–	–
Deafness	+[a]	–	NA
Karyotype	46,XY	46,XY	46,XX

[a]The deafness in patient 1 is conductive because of recurrent otitis media.
KDM6A gene variants were deposited in a gene-specific database (http://www.lovd.Nl/KDM6A).
NA, not analyzed.

in female mice was not twice that in male mice [Xu et al., 2008]. In addition, *UTY* (Yq11.221), a paralog of *KDM6*, has been suspected to partially compensate in males while its function is not well known [Lederer et al., 2012; Xu et al., 2008]. Patient 3 in our study showed a random pattern of X-inactivation with the ratio 57:43 in genomic DNA of peripheral leukocytes. Interestingly, marked skewing of X-inactivation was observed in two female patients reported by Lederer et al. (2012). In their lymphoblast, *KDM6A* deletion was recognized at inactive X chromosome in all 70 mitoses. Here, we propose the threshold model for the pathogenicity of *KDM6A* abnormality (Supp. Fig. S1). The two female patients with a *KDM6A* deletion might not attain the appropriate level of *KDM6A* expression allowing normal development due to existence of specific cells with unfavorable inactivation, whereas male and pure Turner syndrome female with appropriate *KDM6A* expression do not show KS phenotype under assumption of unknown partial functional compensation of *KDM6A* by *UTY* in Y chromosome (only for male) (Supp. Fig. S1).

We reviewed the clinical details of the three patients (Table 1; Supp. Text). All patients were born to unrelated healthy parents. All the three showed severe developmental delay and intellectual disability. Interestingly, patient 3 (female) presented less dysmorphic features and the two male patients 1 and 2 showed a much more severe phenotype with multiple organ involvement (Table 1; Fig. 1E). Null expression of *KDM6A* in males and residual *KDM6A* expression from active X chromosome may explain sex-biased severity (Supp. Fig. S1). Alternatively, it could be explained by a lesser effect of the in-frame mutation in female patient. However, in a previous study, the severity of clinical symptoms varied also among two female patients and a male with a *KDM6A* deletion [Lederer et al., 2012]. More studies of KS patients with *KDM6A* abnormality are necessary. It is likely that the mutation type as well as the X-inactivation pattern in affected organs in females may determine the severity of KS.

In conclusion, we have described the first three point mutations of *KDM6A* in KS. Our three patients out of 32 *MLL2*-negative patients (mutation detection rate: 9.3%) are comparable to the three patients out of 22 *MLL2*-negative patients (13.6%) previously described [Lederer et al., 2012], regardless of the mutation type. The mutation detection rates for *MLL2* (55–80%) plus *KDM6A* (9–13%) in KS suggest that other gene(s) may be found. Because both MLL2 and KDM6A are histone modifiers, the other pathogenic genes might have related functions. Further research is needed to understand the pathomechanisms of KS as well as the role of histone modification in human disease.

Acknowledgments

We thank the patients and their families for participating in this work. We also thank Ms. Y. Yamashita and Ms. S. Sugimoto for technical assistance.

References

Banka S, Veeramachaneni R, Reardon W, Howard E, Bunstone S, Ragge N, Parker MJ, Crow YJ, Kerr B, Kingston H, Metcalfe K, Chandler K, et al. 2012. How genetically heterogeneous is Kabuki syndrome? MLL2 testing in 116 patients, review and analyses of mutation and phenotypic spectrum. Eur J Hum Genet 20:381–388.

Bianca S, Barrano B, Cataliotti A, Indaco L, Ingegnosi C, Ettore G. 2009. Kabuki syndrome and sex chromosomal anomalies: is it really an association? Fertil Steril 91:e6.

Dennis NR, Collins AL, Crolla JA, Cockwell AE, Fisher AM, Jacobs PA. 1993. Three patients with ring (X) chromosomes and a severe phenotype. J Med Genet 30:482–486.

Greenfield A, Carrel L, Pennisi D, Philippe C, Quaderi N, Siggers P, Steiner K, Tam PP, Monaco AP, Willard HF, Koopman P. 1998. The UTX gene escapes X inactivation in mice and humans. Hum Mol Genet 7:737–742.

Kuroki Y, Suzuki Y, Chyo H, Hata A, Matsui I. 1981. A new malformation syndrome of long palpebral fissures, large ears, depressed nasal tip, and skeletal anomalies associated with postnatal dwarfism and mental retardation. J Pediatr 99:570–573.

Lederer D, Grisart B, Digilio MC, Benoit V, Crespin M, Ghariani SC, Maystadt I, Dallapiccola B, Verellen-Dumoulin C. 2012. Deletion of KDM6A, a histone demethylase interacting with MLL2, in three patients with Kabuki syndrome. Am J Hum Genet 90:119–124.

Lee MG, Villa R, Trojer P, Norman J, Yan KP, Reinberg D, Di Croce L, Shiekhattar R. 2007. Demethylation of H3K27 regulates polycomb recruitment and H2A ubiquitination. Science 318:447–450.

Matsumoto N, Niikawa N. 2003. Kabuki make-up syndrome: a review. Am J Med Genet 117C:57–65.

McGinniss MJ, Brown DH, Burke LW, Mascarello JT, Jones MC. 1997. Ring chromosome X in a child with manifestations of Kabuki syndrome. Am J Med Genet 70:37–42.

Niikawa N, Kuroki Y, Kajii T, Matsuura N, Ishikiriyama S, Tonoki H, Ishikawa N, Yamada Y, Fujita M, Umemoto H, Iwama Y, Kondoh I, et al. 1988. Kabuki make-up (Niikawa–Kuroki) syndrome: a study of 62 patients. Am J Med Genet 31:565–589.

Niikawa N, Matsuura N, Fukushima Y, Ohsawa T, Kajii T. 1981. Kabuki make-up syndrome: a syndrome of mental retardation, unusual facies, large and protruding ears, and postnatal growth deficiency. J Pediatr 99:565–569.

Rodriguez L, Diego-Alvarez D, Lorda-Sanchez I, Gallardo FL, Martinez-Fernandez ML, Arroyo-Munoz ME, Martinez-Frias ML. 2008. A small and active ring X chromosome in a female with features of Kabuki syndrome. Am J Med Genet 146A:2816–21.

Sengoku T, Yokoyama S. 2011. Structural basis for histone H3 Lys 27 demethylation by UTX/KDM6A. Genes Dev 25:2266–2277.

Stankiewicz P, Thiele H, Giannakudis I, Schlicker M, Baldermann C, Kruger A, Dorr S, Starke H, Hansmann I. 2001. Kabuki syndrome-like features associated with a small ring chromosome X and XIST gene expression. Am J Med Genet 102:286–292.

Wellesley DG, Slaney S. 1994. Kabuki make-up and Turner syndromes in the same patient. Clin Dysmorphol 3:297–300.

Xu J, Deng X, Watkins R, Disteche CM. 2008. Sex-specific differences in expression of histone demethylases Utx and Uty in mouse brain and neurons. J Neurosci 28:4521–4527.

ORIGINAL ARTICLE

PAPSS2 mutations cause autosomal recessive brachyolmia

Noriko Miyake,[1] Nursel H Elcioglu,[2] Aritoshi Iida,[3] Pinar Isguven,[4] Jin Dai,[3] Nobuyuki Murakami,[5] Kazuyuki Takamura,[6] Tae-Joon Cho,[7] Ok-Hwa Kim,[8] Tomonobu Hasegawa,[9] Toshiro Nagai,[5] Hirofumi Ohashi,[10] Gen Nishimura,[11] Naomichi Matsumoto,[1] Shiro Ikegawa[3]

[1]Department of Human Genetics, Yokohama City University Graduate School of Medicine, Yokohama, Japan
[2]Department of Pediatric Genetics, Marmara University Pendik Hospital, Istanbul, Turkey
[3]Laboratory for Bone and Joint Diseases, Center for Genomic Medicine, RIKEN, Tokyo, Japan
[4]Department of Pediatrics and Pediatric Endocrinology, Medeniyet University Goztepe Hospital, Istanbul, Turkey
[5]Department of Pediatrics, Dokkyo Medical University Koshigaya Hospital, Koshigaya, Japan
[6]Department of Orthopaedic Surgery, Fukuoka Children's Hospital, Fukuoka, Japan
[7]Division of Pediatric Orthopaedics, Seoul National University Children's Hospital, Seoul, Korea
[8]Department of Radiology, Ajou University Hospital, Suwon, Korea
[9]Department of Pediatrics, Keio University School of Medicine, Tokyo, Japan
[10]Division of Medical Genetics, Saitama Children's Medical Center, Saitama, Japan
[11]Department of Pediatric Imaging, Tokyo Metropolitan Children's Medical Center, Futyu, Japan

Correspondence to
Noriko Miyake, Department of Human Genetics, Yokohama City University Graduate School of Medicine, 3-9, Fukuura, Kanazawa-ku, Yokohama 236-0004, Japan; nmiyake@yokohama-cu.ac.jp or Shiro Ikegawa, Laboratory of Bone and Joint Diseases, Center for Genomic Medicine, RIKEN 4-6-1 Shirokanedai, Minato-ku, Tokyo 108-8639, Japan; sikegawa@ims.u-tokyo.ac.jp

NM, NHE and AI contributed equally to this work.

Received 8 May 2012
Revised 8 June 2012
Accepted 10 June 2012

ABSTRACT

Background Brachyolmia is a heterogeneous group of skeletal dysplasias that primarily affects the spine. Clinical and genetic heterogeneity have been reported; at least three types of brachyolmia are known. *TRPV4* mutations have been identified in an autosomal dominant form of brachyolmia; however, disease genes for autosomal recessive (AR) forms remain totally unknown. We conducted a study on a Turkish family with an AR brachyolmia, with the aim of identifying a disease gene for AR brachyolmia.

Methods and results We examined three affected individuals of the family using exon capture followed by next generation sequencing and identified its disease gene, *PAPSS2* (phosphoadenosine-phosphosulfate synthetase 2). The patients had a homozygous loss of function mutation, c.337_338insG (p.A113GfsX18). We further examined three patients with similar brachyolmia phenotypes (two Japanese and a Korean) and also identified loss of function mutations in *PAPSS2*; one patient was homozygous for IVS3+2delT, and the other two were compound heterozygotes for c.616-634del19 (p.V206SfsX9) and c.1309-1310delAG (p.R437GfsX19), and c.480_481insCGTA (p.K161RfsX6) and c.661delA (p.I221SfsX40), respectively. The six patients had short-trunk short stature that became conspicuous during childhood with normal intelligence and facies. Their radiographic features included rectangular vertebral bodies with irregular endplates and narrow intervertebral discs, precocious calcification of rib cartilages, short femoral neck, and mildly shortened metacarpals. Spinal changes were very similar among the six patients; however, epiphyseal and metaphyseal changes of the tubular bones were variable.

Conclusions We identified *PAPSS2* as the disease gene for an AR brachyolmia. *PAPSS2* mutations have produced a skeletal dysplasia family, with a gradation of phenotypes ranging from brachyolmia to spondylo-epi-metaphyseal dysplasia.

INTRODUCTION

Brachyolmia is a heterogeneous group of skeletal dysplasias that primarily affects the spine. The name comes from the Greek for 'short trunk'; patients with brachyolmia have short stature due to a short trunk.[1] Conceptually, skeletal lesions of brachyolmia are limited to the spine; however, it is generally thought that pure brachyolmia (spine-only dysplasia) does not exist and that metaphyseal and/or epiphyseal involvements may be minimal and scattered, but are always present along with spinal involvements in cases labelled brachyolmia.[2]

Clinical and genetic heterogeneity have been reported in brachyolmia. At least three relatively well defined types of brachyolmia are known: type 1 that includes the Hobaek (OMIM 271530) and Toledo (OMIM 271630) forms; type 2 (OMIM 613678) referred to as the Maroteaux type; and type 3 (OMIM 113500). The former two types are autosomal recessive (AR) traits, while the latter is an autosomal dominant trait. Type 1 is characterised by scoliosis, platyspondyly with rectangular and elongated vertebral bodies, overfaced pedicles, and irregular and narrow intervertebral spaces. The Toledo form is distinguished from the Hobaek form by the presence of corneal opacity and precocious calcification of the costal cartilage.[3 4] Type 2 is distinguished by rounded vertebral bodies, less overfaced pedicles, minor facial anomalies, and precocious calcification of the falx cerebri.[1] Type 3 is characterised by severe kyphoscoliosis and flattened, irregular cervical vertebrae. Heterozygous mutations in the *TRPV4* (transient receptor potential vanilloid 4) gene (OMIM 605427) have been identified in several patients with type 3, autosomal dominant brachyolmia;[5 6] however, disease genes for recessive forms of brachyolmia remain totally unknown.

To identify novel disease genes from a limited number of subjects, exome sequencing (exon capture followed by next generation sequencing) is a promising approach. This approach sometimes presents us with unusual and unexpected connection between genes and phenotypes, thereby opening a new window for biology and medicine. We experienced a family with an AR form of brachyolmia harbouring three affected individuals. By performing exome sequencing for the family, we have identified the disease gene for the recessive brachyolmia, *PAPSS2* (phosphoadenosine-phosphosulfate synthetase 2). The discovery was confirmed by identification of *PAPSS2* mutations in three sporadic patients with different ethnic backgrounds but similar brachyolmia phenotypes. All patients had loss of function mutations of *PAPSS2* in both chromosomes.

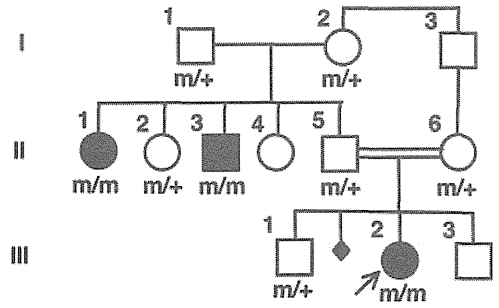

Figure 1 The pedigree of family 1 and co-segregation of the *PAPSS2* mutation (c.337_338insG) in the family. m: mutation allele, +: wild type allele.

MATERIALS AND METHODS

Subjects

P1-3 (family 1)

The proband (P1; III-2 in figure 1) was a Turkish girl referred to one of us (NHE) for genetic evaluation at the age of 8 years 4 months. She has been followed up for her spinal deformity and lumber pain elsewhere for 5 years. She was the result of a consanguineous (first cousin) marriage. A paternal uncle (P2; II-3 in figure 1) and aunt (P3; II-1 in figure 1) had the similar disease (table 1). The paternal grandparents originated from a small area and could be related. The inheritance of the disease was consistent with AR mode. Her birth length was 49 cm and weight 2800 g. She did not gain well after birth and was investigated for short stature at the age of 1 year. Her back deformity was noticed at around 3 years of age. On examination, she had short-trunk short stature. Her height was 109 cm (−3.2 SD), weight 29 kg (+0.38 SD) and head circumference 51 cm (−0.6 SD). She was mentally normal with no hearing or vision problems. She had widened wrists, bulbous proximal interphalangeal joints, clinodactyly of the fifth finger, and bowing deformity in her left lower leg. Serum DHEA-S (dehydroepiandrosterone-sulfate) was under the detection limit (<15.0 μg/dl).

Repeated skeletal surveys showed definite spondylodysplasia with minimal epiphyseal and metaphyseal changes, which was compatible with brachyolmia (table 1 and figure 2). Vertebral bodies were flat, particularly in thoracic spines. Endplates were irregular and intervertebral disc spaces were narrowed. The acetabular roof was horizontal. Femoral necks were slightly short. Metaphyses of the distal tibias had striation. Metacarpals were mildly shortened with mild metaphyseal changes. The bone age was advanced; 6 years 10 months at chronological age 5 years 8 months, and 10 years at chronological age 8 years 2 months (Greulich-Pyle method). MRIs and CTs showed no calcification of the falx cerebri.

At her last visit (10 years 4 months old), she had increasing back deformity and pain. Her height was 121 cm (−3.4 SD), arm span 119 cm, and sitting/standing height ratio was 0.53.

Table 1 Clinical and radiographic phenotypes of autosomal recessive brachyolmina harbouring *PAPSS2* mutation (in comparison to those in spondylo-epi-metaphyseal dysplasia Pakistani type)

Patient ID	P1	P2	P3	P4	P5	P6	
Family	Family 1						
Intra-family ID	III-2	II-3	II-1	Family 2	Family 3	Family 4	Patient reported by Noordam *et al*
Country of origin	Turkey			Japan	Japan	Korea	Turkey
Sex	Female	Male	Female	Female	Female	Male	Female
Age at first presentation	8 years 4 months	29 years	40 years	11 years 4 months	8 years 8 months	12 years 7 months	8 years
Birth length (cm)	49	NA	NA	46	47	50	NA
Birth weight (g)	2800	NA	NA	3340	2676	3100	NA
Consanguinity of the parents	+	Probably +	Probably +	(−)	(−)	(−)	(−)
Clinical feature							
Normal intelligence	+	+	+	+	+	+	NA
Normal facies	+	+	+	+	+	+	NA
Short-trunk short stature	+	+	+	+	+	+	+
Spinal deformity	Kyphosis	(−)	Kyphosis, lumbar scoliosis	Kyphosis	(−)	(−)	Lumbar scoliosis
Leg deformity	Bil genu varum and internal rotation	(−)	Bil genu varum and internal rotation	(−)	Right genu valgum	Bil genu varum	NA
Androgen excess sign	(−)	(−)	(−)	(−)	(−)	(−)	+
Radiographic feature							
Rectangular vertebra	+	+	+	+	+	+	+
Irregular endplate	+	+	+	+	+	+	+
Narrowed disc	+	+	+	+	+	+	+
Precocious calcification of costal cartilage	(−)	+	+	+	(−)	(−)	NA
Delayed ossification of hip and knee epiphyses	(−)	NA	NA	(−)	(−)	(−)	(−)
Early osteoarthritic change	(−)*	(−)	(−)	(−)	(−)*	(−)*	(−)*
Short femoral neck	+	+	+	+	+	+	+
Metaphyseal abnormality†	Dist tibia	Prox tibia	Prox tibia	(−)	(−)	Prox tibia	(−)
Mild brachymetacarpia	+	+	+	+	+	+	+
Advanced bone age	+	NA	NA	+	+	+	+

*May be too young to be evaluated.
†Other than short femoral neck and fingers.
Bil, bilateral; Dist, distal; NA, not available or assessed; Prox, proximal.

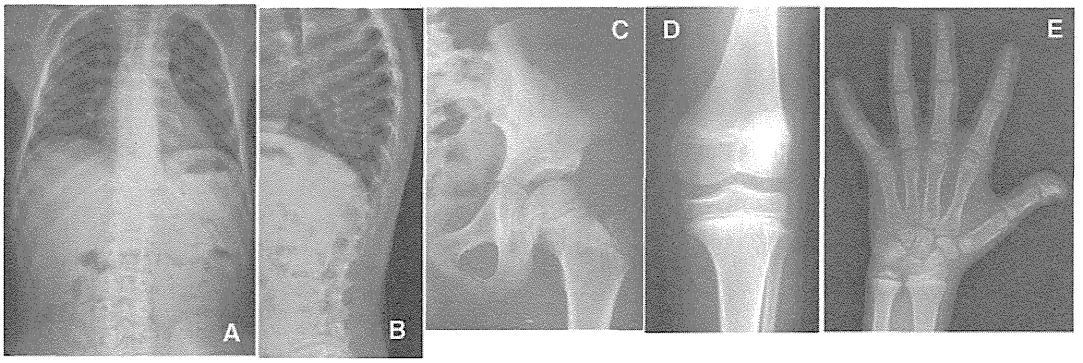

Figure 2 Radiographs of P1 (III-2 in family 1) at age 8.5 years. (A) Spine anteroposterior (AP). Mildly overfaced vertebra. (B) Lateral spine. Mild flattening of vertebral bodies and irregular endplates. (C) Left hip AP. Almost normal epiphysis. (D) Left knee AP. Epiphyseal and metaphyseal abnormalities are unremarkable. (E) Left hand AP. Metacarpals are mildly shortened with mild irregularity of the growth plates. Epiphyses of the distal radius and ulna show mild dysplasia. The bone age is advanced.

Breast development was Tanner 2–3, pubic hair Tanner 1. There had been no sign of androgen excess (acne, hirsutism, etc).

P4-6 (sporadic cases)

After we found *PAPSS2* mutations in family 1, we reviewed the patient registry of the Japanese Skeletal Dysplasia Consortium and found two Japanese patients (P4-5) and one Korean patient (P6) who had similar phenotypes to those of the Turkish family (table 1 and figure 3); all three were sporadic cases from normal, non-consanguineous parents and were *TRPV4* mutation negative.

DNA sample

Genomic DNA was extracted by standard procedures from peripheral blood of the patients and/or their family members after informed consent. The study was approved by the ethical committee of RIKEN, Yokohama City University, and participating institutions.

Exome sequencing

Three affected individuals of family 1 (II-1, II-3 and III-2) were analysed by whole exome sequencing as previously reported (see supplementary online table S1).[7 8] In brief, 3 μg of genomic DNA was sheared by Covaris S2 system (Covaris, Woburn, Massachusetts, USA) and processed using a SureSelect Human All Exon 50 Mb Kit (Agilent Technologies, Santa Clara, California, USA) according to the manufacturer's instructions. DNAs were captured by the kit and were sequenced by GAIIx (Illumina, San Diego, California, USA) with 108 pair-ends reads. Each sample was run in one lane. Image analysis and base calling were performed by sequence control software 2.9 and real time analysis 1.9 (Illumina), and CASAVA software V.1.8.1 (Illumina). The quality-controlled (path-filtered) reads were mapped to human genome reference hg19 with Mapping and Assembly with Qualities (MAQ, http://maq.sourceforge.net/) and NextGENe software V.2.00 (SoftGenetics, State College, Pennsylvania, USA). The variants from MAQ were annotated by SeattleSeq annotation 131 (http://snp.gs.washington.edu/SeattleSeqAnnotation131/).

Priority scheme

Variants were filtered by the following conditions using the script created by BITS (Tokyo, Japan): (1) variants only annotated on human autosomes and chromosome X; (2) variants not in dbSNP131, dbSNP134, the 1000 Genomes database (http://www.1000genomes.org/), and in-house exome data of normal Japanese controls (n=66); (3) variants that were non-synonymous and intronic changes (±20 bp from exon/intron boundaries) called in common by NextGENe and MAQ, and variants of insertion/deletion with a NextGENe score ≥10. The variant numbers in each category are shown in supplementary online table S1.

Sanger sequencing and evaluation of mutations

To confirm the sequence change identified in P1-3 by the exome sequencing, exon 3 of *PAPSS2* and its flanking intronic sequences (The GenBank reference sequence: NM_001015880) were amplified by PCR from genomic DNA. To examine *PAPSS2* mutation in P4-6, all exons of *PAPSS2* and its flanking intronic sequences were amplified by PCR from genomic DNA. Primer sequences and PCR conditions were as previously described.[9] PCR products were directly sequenced using ABI Prism automated sequencers 3730 (PE Biosystems, Foster City, CA, USA).

To evaluate the possibility of polymorphisms, identified sequence changes were genotyped in 93 ethnically matched controls using the invader assay coupled with PCR as described previously.[10] The sequence changes were evaluated by public databases including OMIM (http://www.ncbi.nlm.nih.gov/omim) and dbSNP (http://www.ncbi.nlm.nih.gov/projects/SNP/).

RESULTS

Exome sequencing

A total of 90 964 194 (II-1), 90 508 738 (II-3) and 90 223 680 (III-2) reads were mapped to the whole human genome in pairs by MAQ. Considering the consanguinity of the family, we focused on the same homozygous mutations shared by the three affected individuals. After filtering, a total of 37 homozygous variants remained as candidates (23 missense, 11 intronic, and three insertion changes) (see supplementary online table S1). Among them, one base pair insertion, c.337_338insG in exon 3 of *PAPSS2*, was highlighted because it is a causative gene for SEMD, Pakistani type (OMIM 612847), that has overlapping features with the phenotypes of the three patients.

The insertion sequence was confirmed by direct sequence of PCR products from genomic DNA. Direct sequencing of nine family members showed co-segregation of the mutation with the disease phenotype (figure 1). The insertion mutation was

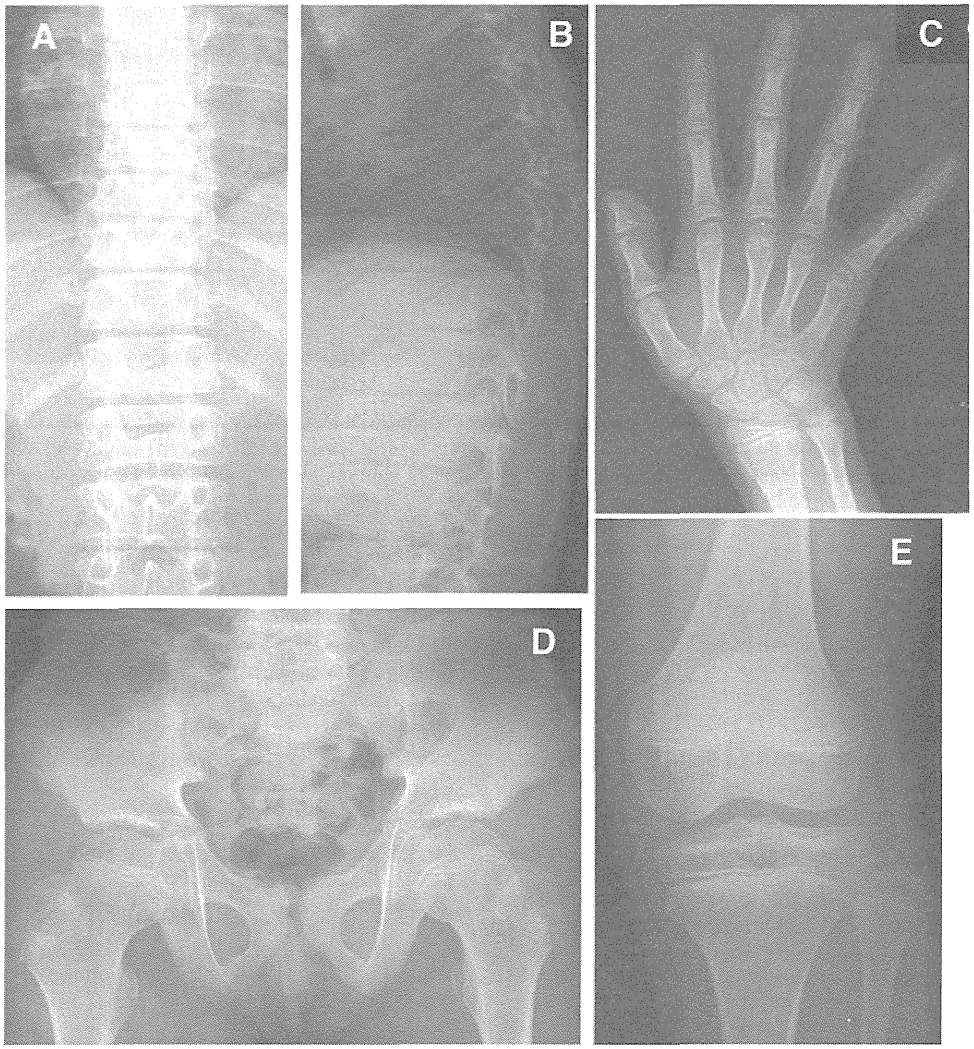

Figure 3 Radiographs of P5 at age 8 years 8 months. (A) Spine anteroposterior (AP). Platyspondyly. Over-faced pedicle is not so distinct. (B) Spine lateral. Flattened vertebral bodies and narrow disc spaces. (C) The right hand AP. Slightly short metacarpals. Phalanges are not so short. The bone age is advanced (12 years by the Greulich-Pyle method). (D) Pelvis AP. Short femoral neck and horizontal acetabulum. Proximal epiphyses are normal. (E) The right knee AP. Unremarkable changes. No fibula overgrowth.

predicted to create a premature stop codon (p.A113GfsX18), thereby most probably resulting in a null allele due to nonsense mutation mediated RNA decay (NMD).[11] The mutation was not found in the public mutation database and sequence variation database. Also, it was not found in 93 ethnically matched controls examined by Invader assay.[10]

Identification of *PAPSS2* mutations in sporadic cases

We screened for *PAPSS2* mutations in P4-6 by direct sequencing as previously described.[9] We found *PAPSS2* mutations in both chromosomes of all subjects (table 2). All mutations are predicted to create premature stop codons before the second last exon of the gene. Therefore, they are most likely to result in null alleles due to NMD. P5 was a homozygote, and P4 and P6 were heterozygotes for the mutations. Compound heterozygosity of the subjects was confirmed by sequencing of the parents' genomic DNA. All these mutations were not found in 93 ethnically matched controls examined by Invader assay[10] nor in public databases.

Phenotypes of the patients with *PAPSS2* mutations

Clinical features of our six patients were short-trunk short stature with short neck (table 1). The short stature was noticeable early in life, but not always at birth; it usually became definite after age 5–6 years. All patients had normal intelligence and facies. Corneal opacity was not found. Kyphosis and/or scoliosis were found in three subjects. Bone age was advanced in all (4/4) cases evaluated. No clinical sign of androgen excess was noted in all (6/6) patients and their family members. The main radiographic feature was pronounced flattening of spine (rectangular vertebral body), particularly in the thoracic spine, which accompanied irregular

Table 2 *PAPSS2* mutations in autosomal recessive brachyolmia

Family	Exon	Nucleotide change	Amino acid change
1	3	c.337_338insG (homozygous)	p.A113GfsX18
2	5	c.616-634del19	p.V206SfsX9
	11	c.1309-1310delAG	p.R437GfsX19
3	3	IVS3+2delT (homozygous)	p.L50SfsX2
4	4	c.480_481insCGTA	p.K161RfsX6
	6	c.661delA	p.I221SfsX40

The nucleotide changes are shown with respect to *PAPSS2* mRNA sequence (NM_001015880). The corresponding predicted amino acid changes are numbered from the initiating methionine residue. Exons are numbered sequentially 1–13.

endplates and narrow disc spaces. Mild shortening of the femoral neck and metacarpals were common features. The costal cartilages showed precocious calcification in the adult subjects (3/3). Epiphyseal and metaphyseal dysplasias were very mild, if present. From these features of spine predominant dysplasia, our patients can be diagnosed as having brachyolmia. Among known types of brachyolmias, characteristics of the Hobaek and Toledo types are mixed.[1 4]

DISCUSSION

PAPSS2 mutation has been reported to be responsible for two other overlapping, but distinct, phenotypes. The first is SEMD Pakistani type; Ahmad *et al*[12] described a large consanguineous Pakistani family with a distinct form of SEMD with autosomal inheritance. Its clinical features include short stature evident at birth, short and bowed lower limbs, mild brachydactyly, kyphoscoliosis, enlarged knee joints, and precocious osteoarthropathy. Radiographic features are platyspondyly with irregular endplates and narrowed joint spaces, delayed epiphyseal ossification at the hips and knees, diffuse early osteoarthritic changes primarily in the spine and hands, and mild brachydactyly. Metaphyseal abnormalities are seen predominantly in the hips and knees. This disease is differentiated from other forms of SEMD by its mild degree of metaphyseal involvement, type of brachydactyly, and the absence of loose joints or other clinical findings. A homozygous nonsense mutation of *PAPSS2* (S438X) is identified in all affected individuals in the family.[13] Many of the characteristics of SEMD Pakistani type, including enlarged joints with deformity, delayed epiphyseal ossification at the hips and knees, and precocious osteoarthritic changes of the large and small joints, are absent in our cases (table 1).

PAPSS2 mutations have also been found in a patient with a different phenotype, spondylodysplasia and premature pubarche.[9] A Turkish girl with premature pubarche, hyperandrogenic anovulation, short stature, and skeletal dysplasia showed a compound heterozygosity for a missense and a nonsense mutation in *PAPSS2*: the former was a 143C>G transversion resulting in a T48R substitution at a conserved residue in the adenosine 5-prime-phosphosulfate kinase domain, and the latter was a 985C>T transition resulting in R329X. Their functional assays revealed no detectable activity for R329X, and only minor residual activity for T48R (6% of the wild type activity). The mother who carried the R329X mutation had normal pubarche and menarche, but developed obesity, oligomenorrhoea, and hirsutism in her fourth decade, while the father who carried the T48R mutation showed normal growth and pubertal development. The skeletal changes in this patient are more similar to those of our cases than SEMD Pakistani type (table 1).

Among our patients, spinal changes were very similar, but epiphyseal and metaphyseal changes were considerably variable (table 1). P4 and P5, similar to the case reported by Noordam *et al*,[9] showed minimal epiphyseal and metaphyseal dysplasias. P6 had considerable epi-metaphyseal changes in the long bones of the lower extremities; they were more severe than those in family 1 (P1-3), but were far milder than those in SEMD Pakistani type. The differential diagnosis includes AR spondyloepiphyseal dysplasia tarda[14] because of late manifestation, AR inheritance, and relatively mild spondyloepiphyseal dysplasia with flat vertebral bodies with irregular endplates. In the disorder, overfaced vertebral bodies is absent and the capital femoral epiphyses are severely affected.[14]

In a form of autosomal dominant brachyolmia, heterozygous *TRPV4* mutation has been identified.[5 6] Notably, the *TRPV4* mutation presents a wide phenotypic gradation from brachyolmia at its most mild, through spondylometaphyseal dysplasia type Kozlowski, spondyloepiphyseal dysplasia type Maroteaux, and metatropic dysplasia, to parastremmatic dysplasia and fetal akinesia at its most severe.[5 15–17] *PAPSS2* mutations might also present a phenotype gradation from brachyolmia to spondylo-epiphyseal and spondylo-epimetaphyseal dysplasia like SEMD Pakistani type. Further investigation of *PAPSS2* mutations in brachyolmia and skeletal dysplasias with overlapping phenotypes to our cases as well as other cases with *PAPSS2* mutations[9 14] would provide further answers.

An additional supplementary table is published online only. To view this file please visit the journal online (http://jmg.bmj.com)

Acknowledgements We thank the patients and their family for their help to the study. We also thank the Japanese Skeletal Dysplasia Consortium.

Contributors NM performed the exome experiments, analysed the data, wrote the paper, and is guarantor. NE and PI collected family samples and evaluated their phenotypes. AI performed the sequence experiments, analysed the data, and wrote the paper. JD performed the experiments. NoM, KM, TC, OK, and TN collected samples and evaluated their clinical and radiographic phenotypes. TH and GN analysed the clinical data. HO collected and controlled the experimental samples. NaM performed the experiments and analysed the data. SI analysed the data, wrote the paper, and is also guarantor. All authors have critically revised the paper.

Funding This study is supported by research grants from the Ministry of Health, Labour and Welfare (23300101: S Ikegawa and N Matsumoto; 23300102: T Hasegawa; 23300201: S Ikegawa), by a Grant-in-Aid for Young Scientists from the Japan Society for the Promotion of Science (N Miyake), and by Research on intractable diseases, Health and Labour Sciences Research Grants, H23-Nanchi-Ippan-123 (S Ikegawa).

Patient consent Obtained.

Ethics approval This study was performed under the approval of the ethical committee of RIKEN, Yokohama City University, and participating institutions.

Provenance and peer review Not commissioned; externally peer reviewed.

Data sharing statement Additional unpublished data on mutation examination are available on request to researchers.

REFERENCES

1. **Shohat M,** Lachman R, Gruber HE, Rimoi DL. Brachyolmia: radiographic and genetic evidence of heterogeneity. *Am J Med Genet* 1989;**33**:209–19.
2. **Kozlowski K,** Beemer FA, Bens G, Dijkstra PF, Iannaccone G, Emons D, Lopez-Ruiz P, Masel J, van Nieuwenhuizen O, Rodriguez-Barrionuevo C. Spondylo-Metaphyseal Dysplasia (Report of 7 cases and essay of classification). *Prog Clin Biol Res* 1982;**104**:89–101.
3. **McKusick VA.** Medical genetics. A 40-year perspective on the evolution of a medical specialty from a basic science. *JAMA* 1993;**270**:2351–6.
4. **Hoo JJ,** Oliphant M. Two sibs with brachyolmia type Hobaek: five year follow-up through puberty. *Am J Med Genet A* 2003;**116A**:80–4.
5. **Rock MJ,** Prenen J, Funari VA, Funari TL, Merriman B, Nelson SF, Lachman RS, Wilcox WR, Reyno S, Quadrelli R, Vaglio A, Owsianik G, Janssens A, Voets T, Ikegawa S, Nagai T, Rimoin DL, Nilius B, Cohn DH. Gain-of-function mutations in TRPV4 cause autosomal dominant brachyolmia. *Nat Genet* 2008;**40**:999–1003.
6. **Dai J,** Cho TJ, Unger S, Lausch E, Nishimura G, Kim OH, Superti-Furga A, Ikegawa S. TRPV4-pathy, a novel channelopathy affecting diverse systems. *J Hum Genet* 2010;**55**:400–2.
7. **Doi H,** Yoshida K, Yasuda T, Fukuda M, Fukuda Y, Morita H, Ikeda S, Kato R, Tsurusaki Y, Miyake N, Saitsu H, Sakai H, Miyatake S, Shiina M, Nukina N, Koyano S, Tsuji S, Kuroiwa Y, Matsumoto N. Exome sequencing reveals a homozygous SYT14 mutation in adult-onset, autosomal-recessive spinocerebellar ataxia with psychomotor retardation. *Am J Hum Genet* 2011;**89**:320–7.
8. **Tsurusaki Y,** Okamoto N, Ohashi H, Kosho T, Imai Y, Hibi-Ko Y, Kaname T, Naritomi K, Kawame H, Wakui K, Fukushima Y, Homma T, Kato M, Hiraki Y, Yamagata T, Yano S, Mizuno S, Sakazume S, Ishii T, Nagai T, Shiina M, Ogata K, Ohta T, Niikawa N, Miyatake S, Okada I, Mizuguchi T, Doi H, Saitsu H, Miyake N, Matsumoto N. Mutations affecting components of the SWI/SNF complex cause Coffin-Siris syndrome. *Nat Genet* 2012;**44**:376–8.
9. **Noordam C,** Dhir V, McNelis JC, Schlereth F, Hanley NA, Krone N, Smeitink JA, Smeets R, Sweep FC, Claahsen-van der Grinten HL, Arlt W. Inactivating PAPSS2 mutations in a patient with premature pubarche. *N Engl J Med* 2009;**360**:2310–18.

10. **Ohnishi Y,** Tanaka T, Ozaki K, Yamada R, Suzuki H, Nakamura Y. A high-throughput SNP typing system for genome-wide association studies. *J Hum Genet* 2001;**46**:471–7.
11. **Holbrook JA,** Neu-Yilik G, Hentze MW, Kulozik AE. Nonsense-mediated decay approaches the clinic. *Nat. Genet* 2004;**36**:801–8.
12. **Ahmad M,** Haque MF, Ahmad W, Abbas H, Haque S, Krakow D, Rimoin DL, Lachman RS, Cohn DH. Distinct, autosomal recessive form of spondyloepimetaphyseal dysplasia segregating in an inbred Pakistani kindred. *Am J Med Genet* 1998;**78**:468–73.
13. **Faiyaz ul Haque M,** King LM, Krakow D, Cantor RM, Rusiniak ME, Swank RT, Superti-Furga A, Haque S, Abbas H, Ahmad W, Ahmad M, Cohn DH. Mutations in orthologous genes in human spondyloepimetaphyseal dysplasia and the brachymorphic mouse. *Nat Genet* 1998;**20**:157–62.
14. **Leroy JG,** Leroy BP, Emmery LV, Messiaen L, Spranger JW. A new type of autosomal recessive spondyloepiphyseal dysplasia tarda. *Am J Med Genet A* 2004;**125A**:49–56.
15. **Krakow D,** Vriens J, Camacho N, Luong P, Deixler H, Funari TL, Bacino CA, Irons MB, Holm IA, Sadler L, Okenfuss EB, Janssens A, Voets T, Rimoin DL, Lachman RS, Nilius B, Cohn DH. Mutations in the gene encoding the calcium-permeable ion channel TRPV4 produce spondylometaphyseal dysplasia, Kozlowski type and metatropic dysplasia. *Am J Hum Genet* 2009;**84**:307–15.
16. **Nishimura G,** Dai J, Lausch E, Unger S, Megarbané A, Kitoh H, Kim OH, Cho TJ, Bedeschi F, Benedicenti F, Mendoza-Londono R, Silengo M, Schmidt-Rimpler M, Spranger J, Zabel B, Ikegawa S, Superti-Furga A. Spondylo-epiphyseal dysplasia, Maroteaux type (pseudo-Morquio syndrome type 2), and parastremmatic dysplasia are caused by TRPV4 mutations. *Am J Med Genet A* 2010;**152A**:1443–9.
17. **Unger S,** Lausch E, Stanzial F, Gillessen-Kaesbach G, Stefanova I, Di Stefano CM, Bertini E, Dionisi-Vici C, Nilius B, Zabel B, Superti-Furga A. Fetal akinesia in metatropic dysplasia: The combined phenotype of chondrodysplasia and neuropathy? *Am J Med Genet A* 2011;**155A**:2860–4.

PAPSS2 mutations cause autosomal recessive brachyolmia

Noriko Miyake, Nursel H Elcioglu, Aritoshi Iida, et al.

J Med Genet 2012 49: 533-538 originally published online July 11, 2012
doi: 10.1136/jmedgenet-2012-101039

Epilepsia, 53(8):1441–1449, 2012
doi: 10.1111/j.1528-1167.2012.03548.x

FULL-LENGTH ORIGINAL RESEARCH

CASK aberrations in male patients with Ohtahara syndrome and cerebellar hypoplasia

*Hirotomo Saitsu, †Mitsuhiro Kato, ‡Hitoshi Osaka, §Nobuko Moriyama, ¶Hideki Horita, *Kiyomi Nishiyama, *Yuriko Yoneda, *Yukiko Kondo, *Yoshinori Tsurusaki, *Hiroshi Doi, *Noriko Miyake, †Kiyoshi Hayasaka, and *Naomichi Matsumoto

*Department of Human Genetics, Yokohama City University Graduate School of Medicine, Kanazawa-ku, Yokohama, Japan; †Department of Pediatrics, Yamagata University Faculty of Medicine, Yamagata, Japan; ‡Division of Neurology, Clinical Research Institute, Kanagawa Children's Medical Center, Minami-ku, Yokohama, Japan; §Department of Pediatrics, Hitachi, Ltd., Hitachinaka General Hospital, Hitachinaka, Japan; and ¶Department of Pediatrics, Ibaraki Disabled Children's Hospital, Mito, Japan

Summary

Purpose: Ohtahara syndrome (OS) is one of the most severe and earliest forms of epilepsy. *STXBP1* and *ARX* mutations have been reported in patients with OS. In this study, we aimed to identify new genes involved in OS by copy number analysis and whole exome sequencing.

Methods: Copy number analysis and whole exome sequencing were performed in 34 and 12 patients with OS, respectively. Fluorescence in situ hybridization, quantitative polymerase chain reaction (PCR), and breakpoint-specific and reverse-transcriptase PCR analyses were performed to characterize a deletion. Immunoblotting using lymphoblastoid cells was done to examine expression of CASK protein.

Key Findings: Genomic microarray analysis revealed a 111-kb deletion involving exon 2 of *CASK* at Xp11.4 in a male patient. The deletion was inherited from his mother, who was somatic mosaic for the deletion. Sequencing of the mutant transcript expressed in lymphoblastoid cell lines derived from the patient confirmed the deletion of exon 2 in the mutant transcript with a premature stop codon. Whole exome sequencing identified another male patient who was harboring a c.1A>G mutation in *CASK*, which occurred de novo. Both patients showed severe cerebellar hypoplasia along with other congenital anomalies such as micrognathia, a high arched palate, and finger anomalies. No CASK protein was detected by immunoblotting in lymphoblastoid cells derived from two patients.

Significance: The detected mutations are highly likely to cause the loss of function of the CASK protein in male individuals. *CASK* mutations have been reported in patients with intellectual disability with microcephaly and pontocerebellar hypoplasia or congenital nystagmus, and those with FG syndrome. Our data expand the clinical spectrum of *CASK* mutations to include OS with cerebellar hypoplasia and congenital anomalies at the most severe end.

KEY WORDS: *CASK*, Ohtahara syndrome, Male, Cerebellar hypoplasia.

Ohtahara syndrome (OS), also known as early infantile epileptic encephalopathy with suppression-burst, is one of the most severe and earliest forms of epilepsy (Ohtahara et al., 1976). It is characterized by early onset of seizures, typically frequent epileptic spasms, seizure intractability, characteristic suppression-burst patterns on electroencephalography (EEG), and poor outcome with severe psychomotor retardation (Djukic et al., 2006; Ohtahara & Yamatogi, 2006). Brain malformations such as cerebral dysgenesis, hemimegalencephaly, Aicardi syndrome, and porencephaly are often associated with OS (Yamatogi & Ohtahara, 2002). However, mutations of the *ARX* and *STXBP1* gene have been reported in individuals with OS who showed no brain malformations, indicating that mutated genes are involved in OS (Kato et al., 2007, 2009; Fullston et al., 2010; Giordano et al., 2010; Saitsu et al., 2008, 2010).

CASK (Genbank accession number NM_003688.3) at Xp11.4 encodes a calcium/calmodulin-dependent serine protein kinase of 921 amino acids belonging to the membrane-associated guanylate kinase protein family (Hsueh, 2006). Accumulating evidence indicates that *CASK* is essential for synapse formation at both presynaptic and postsynaptic junctions. In addition, CASK enters the nucleus and regulates expression of genes involved in cortical development (Hsueh, 2006). Recently, heterozygous loss-of-function mutations in *CASK* were found in four female patients with X-linked intellectual disability (ID);

Accepted April 23, 2012; Early View publication June 18, 2012.
Address correspondence to Hirotomo Saitsu, Department of Human Genetics, Yokohama City University Graduate School of Medicine, 3-9 Fukuura, Kanazawa-ku, Yokohama 236-0004, Japan. E-mail: hsaitsu@yokohama-cu.ac.jp

microcephaly and pontocerebellar hypoplasia (MICPCH) and a hemizygous synonymous c.915G>A mutation, which caused skipping of exon 9 of *CASK* in about 20% of the mutant transcripts, was found in a male patient with the same disease and presentation (Najm et al., 2008). To date, 32 additional female cases have been reported, suggesting that ID, MICPCH, growth retardation, axial hypotonia with or without hypertonia of extremities, and optic nerve hypoplasia are caused by loss-of-function mutations of *CASK* in female cases (Moog et al., 2011; Hayashi et al., 2012). On the other hand, a missense mutation causing a partial skipping of exon 2 of *CASK* was found in affected male individuals in an Italian family with FG syndrome, which is characterized by multiple congenital anomalies and ID (Piluso et al., 2009). More recently, five missense mutations and a splice mutation, causing amino acid changes or in-frame deletions of the CASK protein, were found in male patients and variably affected carrier female patients with ID, often accompanied by congenital nystagmus (Tarpey et al., 2009; Hackett et al., 2010). Therefore it has been postulated that hypomorphic *CASK* alleles cause ID in male individuals. Collectively, mutations of *CASK* could cause a wide spectrum of ID, ranging from nonsyndromic mild ID to syndromic severe ID with structural brain abnormalities in both male and female patients.

Herein, we report on two male patients with OS, cerebellar hypoplasia, and multiple congenital anomalies. One patient had a *CASK* deletion and the other had a mutation at the translation initiation codon, both likely leading to a loss of CASK function. Detailed clinical and molecular data are presented.

Methods

Patients

A total of 34 Japanese patients (20 male and 14 female) with OS were analyzed for copy number aberrations. Twelve of them were additionally analyzed by whole exome sequencing. The diagnosis was made based on clinical features and characteristic patterns on EEG. Mutations in *STXBP1* were not identified in these patients (including Patients 1 and 2) by high-resolution melting analysis. Thirteen male patients, including Patient 1, and three female Patients were negative for *ARX* mutation. The experimental protocols were approved by the Yokohama City University School of Medicine Institutional Review Boards for Ethical Issues. Written informed consent was obtained from all individuals and/or their families in compliance with the relevant Japanese regulations.

Genomic microarray and cloning of deletion breakpoint

Genomic DNA obtained from peripheral blood leukocytes was used. Copy number alterations were studied by using Cytogenetics Whole-Genome 2.7M Array (Affymetrix, Santa Clara, CA, U.S.A.) for 30 patients and GeneChip Human Mapping 250K NspI (Affymetrix) for four patients. Copy number alterations were analyzed using the Chromosome Analysis Suite (ChAS; Affymetrix) with NA30.1 (hg18) annotations (for 2.7M Array) or using CNAG2.0 (for 250K) (Nannya et al., 2005). The junction fragment spanning the deletion was amplified by long polymerase chain reaction (PCR), using several primer sets based on putative breakpoints from the microarray data. The junction fragment was amplified using following primers: forward, 5′-ACCCAGCGTTTCACCAAGGTCTCT-3′; reverse, 5′-GTGGCTTCAGAATTAGGCCCACAAA-3′ (product size = 1,136 bp). PCR products were electrophoresed in agarose gels, stained with ethidium bromide, extracted from the gels using a QIAquick Gel extraction kit (Qiagen, Tokyo, Japan), and sequenced.

Quantitative real-time PCR

The deletion of *CASK* was analyzed using the patient's and parental genomic DNA by quantitative real-time PCR (qPCR) on a Rotor-Gene Q thermal cycling system (Qiagen). DNA extracted from two independent blood samples each from the patient and mother were used for analysis. PCR was performed in a volume of 15 μl containing 10 ng of genomic DNA, 1× Rotor-Gene SYBR Green PCR Master Mix (Qiagen), and 1.0 μM each primer. qPCR was carried out using the two standard curve relative quantification method with four standard samples including 30, 10, 3.33, and 1.11 ng DNA, respectively. Three primer sets for exons 2, 3, and 4 of *CASK*, and one reference primer set for an area on chromosome 9 were used. Relative copy number of test regions was calculated in comparison with that of the reference region. The experiments were independently repeated three times. The data were averaged, and the standard deviation was calculated. Primer information is available on request.

Fluorescent in situ hybridization (FISH)

RP11-977L20 covering the deletion of *CASK* was labeled with SpectrumGreen -11-dUTP (Abbott, Tokyo, Japan) by nick translation. Probe-hybridization mixtures (15 μl) were denatured at 70°C for 5 min, applied to chromosomes, incubated at 37°C for 20 h, and then washed and mounted with antifade solution (Vector Laboratories, Burlingame, CA, U.S.A.) containing 4,6-diamidino-2-phenylindole. Photographs were taken on an AxioCam MR Charge Coupled Device camera fitted to an Axioplan2 fluorescence microscope (Carl Zeiss, Tokyo, Japan). The mosaic ratio was examined by two independent investigators, who each counted 100 interphase nuclei.

RNA analysis

RNA analysis using lymphoblastoid cell lines was performed as described previously (Saitsu et al., 2011). Briefly, total RNA was extracted using an RNeasy Plus Mini Kit (Qiagen); 2 μg of total RNA was subjected to reverse transcription, and 1 μl of cDNA was used for PCR.

Primer sequences are ex1-F (5′-ATGTGTACGAGCTGT GCGAGGTGAT-3′) and ex4-R (5′-AGCGTCAGCTCGCT TTACGATTTCA-3′). Two separately extracted RNA samples were used in each duplicated experiment. The DNA in each PCR band was purified using a QIAquick Gel extraction kit (Qiagen) and sequenced.

Whole exome sequencing

DNAs were captured using the SureSelect^{XT} Human All Exon 50 Mb Kit (Agilent Technologies, Santa Clara, CA, U.S.A.) and sequenced with one lane per sample on an Illumina GAIIx platform (Illumina, San Diego, CA, U.S.A.) with 108-bp paired-end reads. Image analysis and base calling were performed by sequence control software real-time analysis and CASAVA software v1.7 (Illumina). A total of 94,106,348 paired-end reads were obtained for Patient 2 and aligned to the human reference genome sequence (GRCh37/hg19) using MAQ (Li et al., 2008) and NextGENe software v2.00 with sequence condensation by consolidation (SoftGenetics, State College, PA, U.S.A.). Single nucleotide variants (SNVs) were called using MAQ and NextGENe. Small insertions and deletions were detected using NextGENe. Called SNVs were annotated with SeattleSeq Annotation. The number of variants identified by exome sequencing in Patient 2 is shown in Table S1.

Immunoblotting

Lymphoblastoid cells were washed twice in ice-cold phosphate-buffered saline (PBS), and lysed in sodium dodecyl sulfate sample buffer. Samples were size-fractionated by sodium dodecyl sulfate–polyacrylamide gel electrophoresis, transferred to the polyvinylidene fluoride membrane, and analyzed with anti-CASK monoclonal antibody, which is produced by a synthetic peptide corresponding to residues surrounding Glu327 of human CASK protein (1:1,000 dilution, D24B12; Cell Signaling, Tokyo, Japan). Anti-Lamin B polyclonal antibody (1:500 dilution, sc-6217; Santa Cruz Biotechnology Inc., Santa Cruz, CA, U.S.A.) was used as a control. Secondary antibody was peroxidase-conjugated goat anti-rabbit IgG or bovine anti-goat IgG (Jackson ImmunoResearch, West Grove, PA, U.S.A.). Blots were detected using the Supersignal West dura (Pierce, Yokohama, Japan). Chemiluminescence was visualized using a FluorChem 8900 (Alpha Innotech, San Leandro, CA, U.S.A.). Experiments were repeated twice using two separately prepared samples.

Results

Clinical information

Patient 1 is a 4-year-old boy born to nonconsanguineous parents. The pregnancy was uneventful, and he was born at term (gestational age 41 weeks and 2 days) with induced labor but no asphyxia. His body weight was 2,606 g (−2.0 standard deviation [SD]), his height was 47.5 cm (−1.4 SD), and his head circumference was 32.2 cm (−1.2 SD). An apneic event with cyanosis, which was not improved by positioning or oxygen inhalation, was evident 2 days after birth. Brain magnetic resonance imaging (MRI) demonstrated prominent cerebellar hypoplasia (Fig. 1A). EEG showed multifocal epileptic discharges with a short period (1 s) of flat basic rhythm (Fig. 1C, left). Phenobarbital was administered at 21 days and was effective for the apneic event. At the age of 2 months, he developed daily clustering of tonic seizures with suppression-burst pattern on both awake and asleep EEG (Fig. 1C, right)and poor feeding. EEG at 5 months demonstrated hypsarrhythmia, which is characteristically seen in West syndrome. He exhibited long slender fingers, micropenis, micrognathia, and a short neck with obstructive respiration, and then required tracheostomy with laryngotracheal separation and gastrostomy. His head circumference was 47.1 cm (−2.7 SD) at 1 years and 4 months. On examination at 4 years, he was bedridden and unable to track objects. Tonic seizures lasting 10–30 s several times a day and frequent myoclonic seizures were seen regardless of treatment with phenobarbital, pyridoxal phosphate, zonisamide, clobazam, and lamotrigine. EEG during sleep at 3 years of age demonstrated multifocal sharp and slow-wave complexes and diffuse low-voltage fast-wave bursts or a desynchronization pattern.

Patient 2 is a 4-year-old boy born to nonconsanguineous parents. He was born at 39 weeks of gestation without asphyxia after uneventful pregnancy. His body weight was 2,000 g (−3.3 SD), his height was 43.0 cm (−2.8 SD), and his head circumference was 29.5 cm (−2.7 SD). He was poorly fed with milk and referred to us at 27 days after birth. Multiple anomalies were recognized such as micrognathia, high arched palate, shortened upper arms, bilateral overlapping fingers and clinodactyly, and persistent hypertrophic primary vitreous. He underwent ophthalmic surgery at 33 days after birth. Brain MRI demonstrated prominent cerebellar hypoplasia (Fig. 1B). At 3 months of age, he showed frequent generalized tonic seizures, and EEG showed a suppression-burst pattern in both awake and asleep states (Fig. 1D). He showed normal auditory brain responses. Laboratory data, including lactate, pyruvate, and very long fatty acids, were all normal. Phenobarbital was initiated and only partially effective for his seizures. Topiramate, clobazam, and sodium bromide were added, and seizure frequencies were decreased from daily to weekly. His development was severely delayed with no head control or eye pursuit. His deep tendon reflexes are exaggerated, with positive bilateral Babinski signs. He shows muscle hypertonus with rigidity of both upper and lower limbs.

Copy number analysis

Through screening for copy number alterations by genomic microarray analysis, we identified an approximately 110-kb microdeletion involving exon 2 of *CASK* at Xp11.4 in Patient 1 (Fig. 2A). Breakpoint-specific PCR analysis of

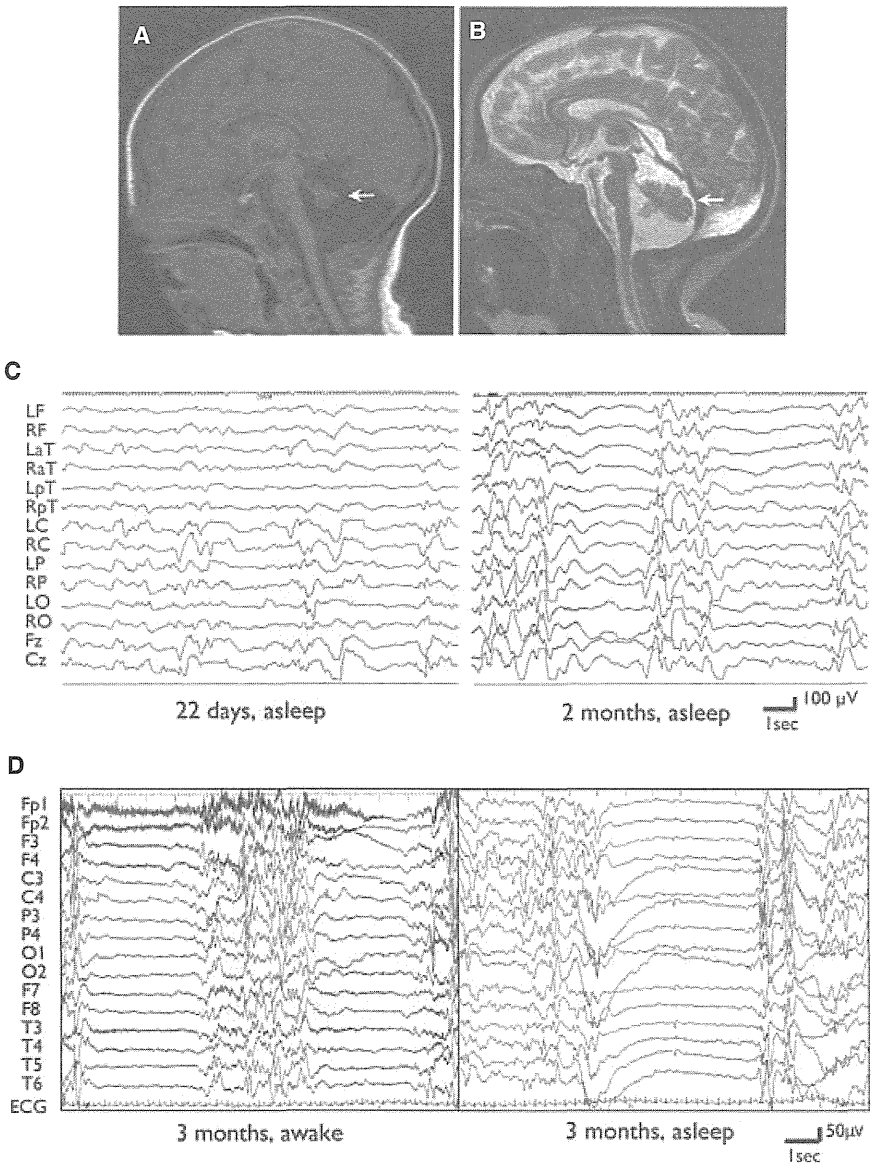

Figure 1.
Brain MRI findings in the patients. (**A**) T_1-weighted midline sagittal image of Patient 1 at age 21 days. (**B**) T_2-weighted midline sagittal image of Patient 2 at age 3 months. Both patients showed prominent cerebellar hypoplasia (arrows). (**C**) EEG of Patient 1 showed multifocal sharp wave or irregular sharp-and-slow wave complex but no diffuse epileptic discharges at age 22 days (left) and diffuse high-amplitude slow-wave burst mixed with irregular spike or sharp wave interrupted by low-amplitude activity (suppression-burst) at age 2 months (right). (**D**) EEG of Patient 2 at age 3 months. High-voltage bursts alternate with almost flat suppression phases at an approximately regular rate in both awake and asleep states.
Epilepsia © ILAE

the family showed that the deletion was inherited from his mother (Fig. 2B). The sequence of the junctional fragment confirmed a 111,172-bp deletion (NG_016754.1: g.17883_129055del) (Fig. 2C). Sequencing also identified 5-bp duplicated sequences as well as a 2-bp insertion at the deletion junction. We were surprised that the healthy mother possessed this deletion, because the deletion is predicted to lead to a frameshift with presumably premature termination of the translation. The deletion was further examined by qPCR and FISH analyses. Whereas the relative copy numbers of exons 3 and 4 (not deleted) were nearly 1.0 in the two maternal DNA samples, as expected, those for deleted exon 2 in the two samples were 0.67 and 0.81 (Fig. 2D). Because the relative copy number is expected to be 0.5 if one of two copies is deleted (as the healthy father showed), this result suggested that the mother may be somatic mosaic for the deletion. In fact, FISH analysis revealed that only 40 of 200 interphase nuclei showed one clear signal and another weaker signal, consistent with partial deletion within the bacterial artificial chromosome probe (Fig. 2E). Based on these findings, we concluded that the mother is somatic mosaic for the deletion, and that the percentage of mosaicism is approximately 20%. To explore the effect of the deletion on the transcription of *CASK*, reverse transcriptase PCR designed to amplify exons 1–4 was performed using total RNA extracted from lymphoblastoid cell lines (LCLs) derived from the patient and his mother (Fig. 2F). A single band (299-bp) corresponding to the wild-type *CASK* allele was amplified using a complementary DNA (cDNA) template from a control LCL (Fig. 2F). By contrast, only a smaller band, in which exon 2 had been deleted, was detected from the patient's cDNA

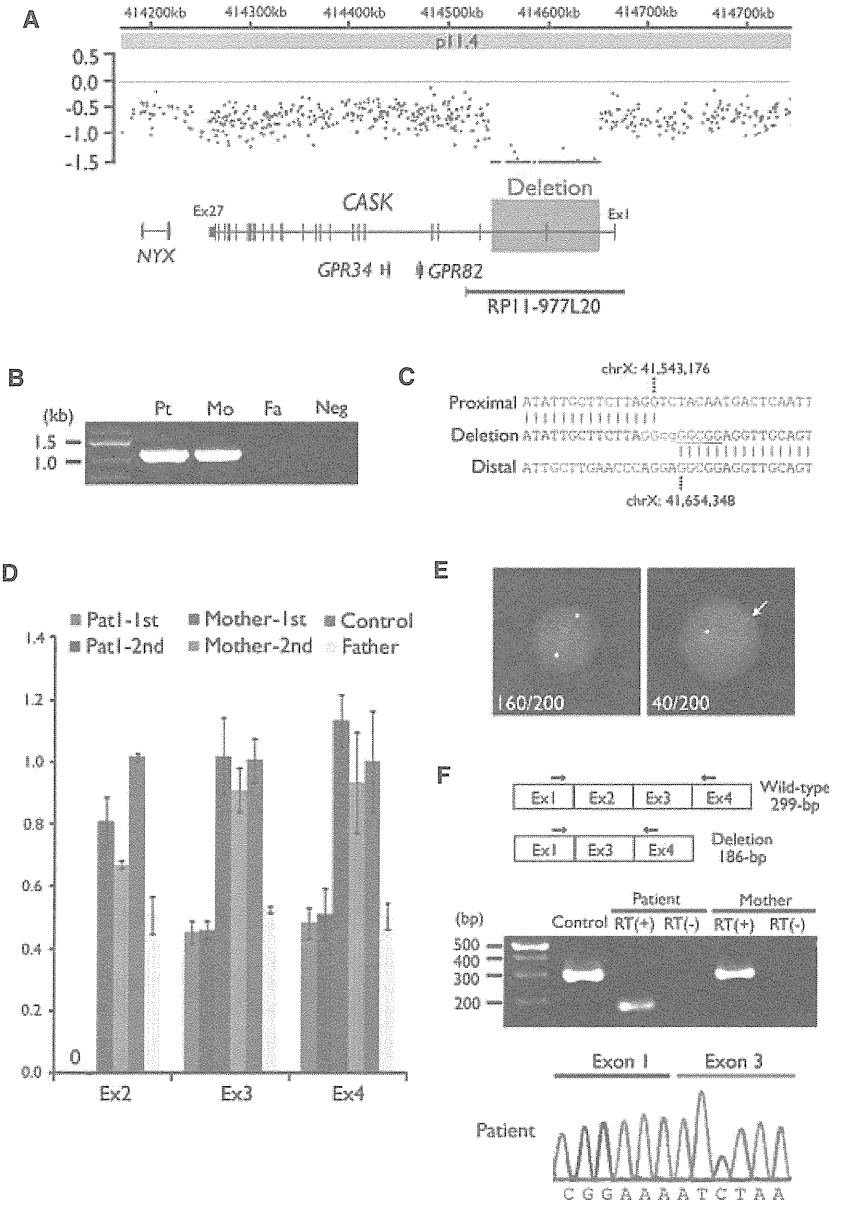

Figure 2.

A 111-kb deletion involving exon 2 of *CASK*. (**A**) The 2.7M array profile clearly shows a deletion involving exon 2 of *CASK* at Xp11.4. The x- and y-axes show the genomic location from the p telomere of chromosome X (UCSC coordinates, May, 2006) and $\log_2$ signal ratio values, respectively. Four RefSeq genes including *CASK* and RP11-977L20 clone used for FISH are shown. (**B**) Breakpoint-specific PCR analysis of the family. Primers flanking the deletion were able to amplify a 1,136-bp product from both the Patient 1 and his mother. Pt, patient; Mo, mother; Fa, Father; Neg, negative control (no template DNA). (**C**) Deletion junction sequence. Top, middle, and bottom strands show proximal, deleted and distal sequences, respectively. The two nucleotides inserted are presented in lower case. A 5-bp sequence that appears twice at the breakpoint region is colored red or underlined. (**D**) qPCR analysis of the family, and a female control. Two DNA samples extracted from two independent blood samples were used for analysis of the patient and his mother. Relative copy numbers of deleted exon 2 were 0.67 and 0.81 (both above 0.5) in the mother, suggesting somatic mosaicism of the deletion. (**E**) FISH images of RP11-977L20, covering the deletion, on the mother's chromosomes. One-hundred sixty nuclei showed two clear signals (left), and 40 nuclei showed one clear signal and a weaker signal (right, white arrow) consistent with partial deletion within the probe. (**F**) Schematic representation of the transcript from exons 1–4 of *CASK*. Exons and primers are depicted as boxes and arrows, respectively (top). A single wild-type amplicon was detected in a control and the mother. A smaller product was amplified only from the patient's cDNA. RT (+): with reverse transcriptase, RT (−): without reverse transcriptase as a negative control. Sequence of a smaller amplicon clearly demonstrated the exon 2 deletion (bottom).

(Fig. 2F). The smaller mutant band was not detected from the mother's cDNA (Fig. 2F). Human androgen receptor assay showed that X-inactivation was random (70:30) in the mother (data not shown). However, because the percentage of mosaicism was low (20%), it remains possible that the deletion allele may undergo X-inactivation in cells possessing it, leading to diminished expression of the deletion allele in LCL.

Whole exome sequencing

To find potential pathologic mutations, whole exome sequencing of 12 patients was performed. We focused on mutations in *CASK*, and identified a hemizygous c.1A>G mutation of the first ATG codon in Patient 2 (Fig. 3A,B). This mutation is anticipated to result in alternative ATG codon usage. By using the next downstream in-frame ATG codon positioned at c.202_204 (Fig. 3C), a truncated protein without the first 67 amino acids containing calmodulin-dependent kinase domain could be produced, although this ATG codon (CATATGC) does not conform to the Kozak consensus. The parental DNA did not have the mutation, suggesting that the mutation occurred de novo (Fig. 3B). No *CASK* mutations were found in any of the other patients.

Immunoblotting

To evaluate mutational effect for CASK expression in two patients, immunoblotting was performed using total lysate of LCL. A strong signal at 104 kDa was detected in a control and the mother of Patient 1, showing strong expression of wild-type CASK protein in LCLs (Fig. 4, top). However, both Patients 1 and 2 did not show any detectable signal (Fig. 4, top), whereas the Lamin B showed comparable expression in all samples loaded (Fig. 4, bottom). Thus these data suggest that expression of CASK protein was severely decreased in two patients.

Discussion

We describe two male patients possessing an intragenic *CASK* deletion (only exon 2) or a hemizygous c.1A>G

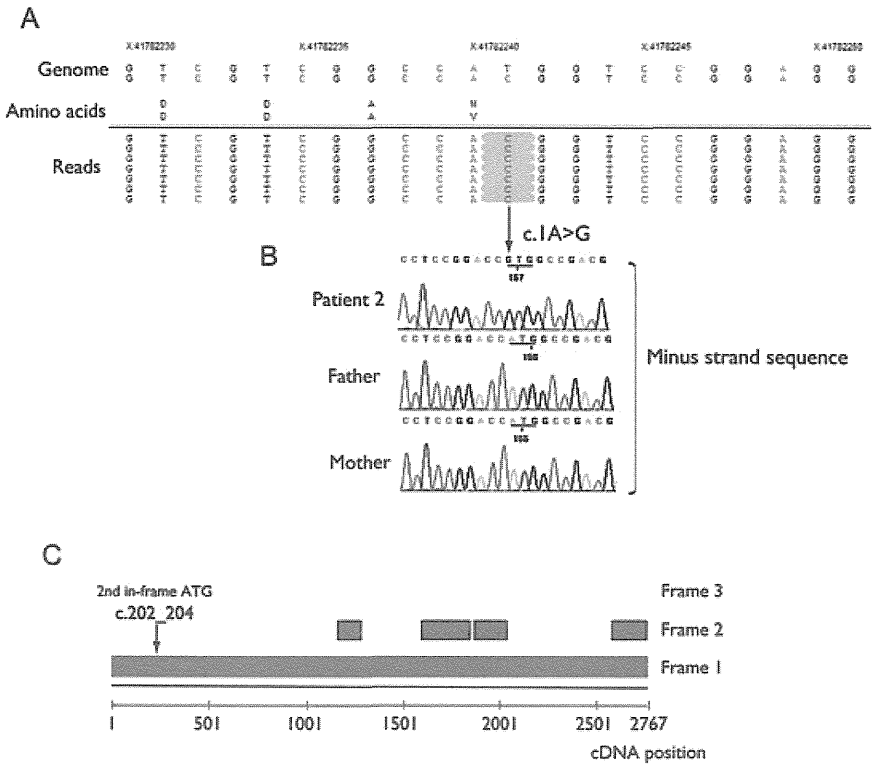

Figure 3.
c.1A>G mutation identified by exome sequencing. (**A**) From top to bottom, genomic sequence (plus strand), coding amino acids, and sequence reads covering the site of the pathogenic mutation. In genomic sequence and amino acids, upper and lower indicate reference and mutant alleles, respectively. There are six reads showing a hemizygous T>C transition at position 41,782,240 of chromosome X. (**B**) Validation of the c.1A>G mutation and inheritance analysis by Sanger sequencing. The mutation position is indicated by the arrow. (**C**) Possible open reading frames within the coding region of the *CASK* transcript (NM_003688.3). Open reading frames longer than 100 bp are shown in blue squares. The second in-frame ATG codon is positioned at c.202_204 (arrow). Any proteins longer than the protein utilizing the second in-frame ATG codon are not predicted.

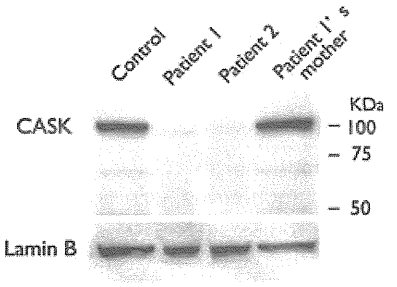

Figure 4.
Expression of CASK protein in LCL. Immunoblot analysis by using a monoclonal CASK antibody (top). Expression of CASK protein was not detected in LCL derived from two patients, whereas LCL of a control and Patient 1's mother showed strong CASK expression. The observed differences in expression were not due to difference of loading conditions, because the level of Lamin B protein was similar in all cases (bottom).

mutation. In Patient 1, the deletion is likely to be an almost null mutation as the mutant *CASK* transcript with exon 2 deletion has a frameshift with premature termination. Deletions in *CASK* have been reported in 16 female patients, and a skewed X-inactivation pattern was observed in two of them (the others had random inactivation pattern or not determined) (Froyen et al., 2007; Hayashi et al., 2008; Najm et al., 2008; Moog et al., 2011; Hayashi et al., 2012). Of interest, partial skipping of the exon 2 of *CASK* (approximately 3–6% of the unskipped transcripts) has been reported in male patients with FG syndrome showing ID, relative macrocephaly, hypotonia, severe constipation, and behavioral disturbance (Piluso et al., 2003, 2009). By contrast, our Patient 1 with complete deletion of exon 2 showed a more severe phenotype, suggesting that he showed one of the most severe phenotypes caused by *CASK* abnormalities. In Patient 2, the mutation of the first ATG codon could produce a truncated protein without the amino terminal 67 amino acids. However, this alternative in-frame ATG codon does not conform to the Kozak consensus, suggesting that its translation would be significantly reduced. In fact, CASK protein was not detected in the LCL of two patients, suggesting that expression of CASK protein should be extremely low. Because only partial skipping of exon 9 (about 20% of the mutant transcripts) (Najm et al., 2008) or of exon 2 (3–6% of the unskipped transcripts) (Piluso et al., 2009) is sufficient to cause ID and other features in male cases, it is likely that the maintenance of expression level of functional CASK protein is essential.

Two male patients with *CASK* abnormalities showed typical OS features, revealing an association between OS and *CASK* abnormalities in male patients, which has to date never been shown. Microcephaly and prominent cerebellar hypoplasia were also recognized, consistent with previous reports (Najm et al., 2008; Moog et al., 2011; Hayashi et al., 2012). Of interest, our patients also showed reduced body size and multiple congenital anomalies such as high arched palate, micrognathia, finger anomalies, and persistent hypertrophic primary vitreous. This suggests that *CASK* may be involved in overall body growth and development of these organs in humans. Supporting this idea, growth retardation and small jaw have been reported in patients with *CASK* abnormalities (Najm et al., 2008; Hackett et al., 2010; Moog et al., 2011). In addition, *CASK*-deficient mice showed micrognathia and cleft palate with male lethality (Laverty & Wilson, 1998), and hypomorphic *CASK* mutant mice are significantly smaller than littermate control mice (Atasoy et al., 2007). Therefore, it is likely that loss-of-function mutations in *CASK* cause reduced body size and multiple congenital anomalies, as well as OS and cerebellar hypoplasia.

The same deletion was found in both the mother and the affected son, indicating a germline mosaicism in the mother associated with recurrence risks. This information is useful for genetic counseling in the family. The maternal somatic mosaicism was confirmed by different methods including FISH, qPCR, and breakpoint-specific PCR analyses. We would like to emphasize the importance of breakpoint-specific PCR analysis, in which a specific band undoubtedly indicates the presence of the deletion allele. Because PCR is a powerful tool for amplifying target sequences, we could easily detect the somatic mosaic, even though it existed in approximately 20% of cells. In addition, it has been reported that PCR analyses of the deletion junction can detect extremely low-level mosaicism not detected by array comparative genomic hybridization (Zhang et al., 2009). The increasing density of available oligonucleotide arrays allows us to design long (or even regular) PCR primers for junctional cloning. Once junctional cloning is successful (though it is sometimes difficult), it is highly useful for examining parental states.

It has been determined that mutations in three genes (*STXBP1*, *ARX*, and *CASK*) cause OS. Screening for *STXBP1* mutations should be considered in OS patients with no brain anomalies in both male and female patients. Screening for *ARX* mutations would be reasonable in male patients with OS, and the presence of micropenis may encourage its screening (Kato et al., 2007). Based on this study, *CASK* mutations should be considered in patients with OS and cerebellar hypoplasia.

In conclusion, we report for the first time *CASK* abnormalities in male individuals with OS. Maternal somatic mosaicism of a *CASK* deletion is also described, suggesting that somatic and germline mosaicism of a microdeletion should be carefully considered in the examination of parental samples. Our data expand the clinical spectrum of *CASK* mutations to include OS with cerebellar hypoplasia and congenital anomalies at the most severe end of clinical presentation.

Acknowledgments

We would like to thank the patients and their families for their participation in this study. This work was supported by Research Grants from the Ministry of Health, Labour and Welfare (H.S., M.K., H.O. N. Miyake, and N. Matsumoto), a Grant-in-Aid for Scientific Research from Japan Society for the Promotion of Science (M.K., H.O., N. Miyake, and N. Matsumoto), a Grant-in-Aid for Young Scientist from Japan Society for the Promotion of Science (H.S., H.D., and N. Miyake), a grant from the Japan Science and Technology Agency (N. Matsumoto), the Strategic Research Program for Brain Sciences (N. Matsumoto), and a Grant-in-Aid for Scientific Research on Innovative Areas (Foundation of Synapse and Neurocircuit Pathology) from the Ministry of Education, Culture, Sports, Science and Technology of Japan (N. Matsumoto), Research Grants from the Japan Epilepsy Research Foundation (H.S. and M.K.), a Research Grant from Naito Foundation (N. Matsumoto), and Research Grants from Takeda Science Foundation (N. Miyake and N. Matsumoto). This work was performed at the Advanced Medical Research Center, Yokohama City University, Japan.

Disclosure

None of the authors has any conflict of interest to disclose. We confirm that we have read the Journal's position on issues involved in ethical publication and affirm that this report is consistent with those guidelines.

References

Atasoy D, Schoch S, Ho A, Nadasy KA, Liu X, Zhang W, Mukherjee K, Nosyreva ED, Fernandez-Chacon R, Missler M, Kavalali ET, Sudhof TC. (2007) Deletion of CASK in mice is lethal and impairs synaptic function. *Proc Natl Acad Sci U S A* 104:2525–2530.

Djukic A, Lado FA, Shinnar S, Moshe SL. (2006) Are early myoclonic encephalopathy (EME) and the Ohtahara syndrome (EIEE) independent of each other? *Epilepsy Res* 70(Suppl. 1):S68–S76.

Froyen G, Van Esch H, Bauters M, Hollanders K, Frints SG, Vermeesch JR, Devriendt K, Fryns JP, Marynen P. (2007) Detection of genomic copy number changes in patients with idiopathic mental retardation by high-resolution X-array-CGH: important role for increased gene dosage of XLMR genes. *Hum Mutat* 28:1034–1042.

Fullston T, Brueton L, Willis T, Philip S, MacPherson L, Finnis M, Gecz J, Morton J. (2010) Ohtahara syndrome in a family with an ARX protein truncation mutation (c.81C>G/p.Y27X). *Eur J Hum Genet* 18:157–162.

Giordano L, Sartori S, Russo S, Accorsi P, Galli J, Tiberti A, Bettella E, Marchi M, Vignoli A, Darra F, Murgia A, Bernardina BD. (2010) Familial Ohtahara syndrome due to a novel *ARX* gene mutation. *Am J Med Genet A* 152A:3133–3137.

Hackett A, Tarpey PS, Licata A, Cox J, Whibley A, Boyle J, Rogers C, Grigg J, Partington M, Stevenson RE, Tolmie J, Yates JR, Turner G, Wilson M, Futreal AP, Corbett M, Shaw M, Gecz J, Raymond FL, Stratton MR, Schwartz CE, Abidi FE. (2010) *CASK* mutations are frequent in males and cause X-linked nystagmus and variable XLMR phenotypes. *Eur J Hum Genet* 18:544–552.

Hayashi S, Mizuno S, Migita O, Okuyama T, Makita Y, Hata A, Imoto I, Inazawa J. (2008) The *CASK* gene harbored in a deletion detected by array-CGH as a potential candidate for a gene causative of X-linked dominant mental retardation. *Am J Med Genet A* 146A:2145–2151.

Hayashi S, Okamoto N, Chinen Y, Takanashi JI, Makita Y, Hata A, Imoto I, Inazawa J. (2012) Novel intragenic duplications and mutations of CASK in patients with mental retardation and microcephaly with pontine and cerebellar hypoplasia (MICPCH). *Hum Genet* 131:99–110.

Hsueh YP. (2006) The role of the MAGUK protein CASK in neural development and synaptic function. *Curr Med Chem* 13:1915–1927.

Kato M, Saitoh S, Kamei A, Shiraishi H, Ueda Y, Akasaka M, Tohyama J, Akasaka N, Hayasaka K. (2007) A longer polyalanine expansion mutation in the *ARX* gene causes early infantile epileptic encephalopathy with suppression-burst pattern (Ohtahara Syndrome). *Am J Hum Genet* 81:361–366.

Kato M, Koyama N, Ohta M, Miura K, Hayasaka K. (2009) Frameshift mutations of the *ARX* gene in familial Ohtahara syndrome. *Epilepsia* 51:1679–1684.

Laverty HG, Wilson JB. (1998) Murine CASK is disrupted in a sex-linked cleft palate mouse mutant. *Genomics* 53:29–41.

Li H, Ruan J, Durbin R. (2008) Mapping short DNA sequencing reads and calling variants using mapping quality scores. *Genome Res* 18:1851–1858.

Moog U, Kutsche K, Kortum F, Chilian B, Bierhals T, Apeshiotis N, Balg S, Chassaing N, Coubes C, Das S, Engels H, Van Esch H, Grasshoff U, Heise M, Isidor B, Jarvis J, Koehler U, Martin T, Oehl-Jaschkowitz B, Ortibus E, Pilz DT, Prabhakar P, Rappold G, Rau I, Rettenberger G, Schluter G, Scott RH, Shoukier M, Wohlleber E, Zirn B, Dobyns WB, Uyanik G. (2011) Phenotypic spectrum associated with CASK loss-of-function mutations. *J Med Genet* 48:741–751.

Najm J, Horn D, Wimplinger I, Golden JA, Chizhikov VV, Sudi J, Christian SL, Ullmann R, Kuechler A, Haas CA, Flubacher A, Charnas LR, Uyanik G, Frank U, Klopocki E, Dobyns WB, Kutsche K. (2008) Mutations of CASK cause an X-linked brain malformation phenotype with microcephaly and hypoplasia of the brainstem and cerebellum. *Nat Genet* 40:1065–1067.

Nannya Y, Sanada M, Nakazaki K, Hosoya N, Wang L, Hangaishi A, Kurokawa M, Chiba S, Bailey DK, Kennedy GC, Ogawa S. (2005) A robust algorithm for copy number detection using high-density oligonucleotide single nucleotide polymorphism genotyping arrays. *Cancer Res* 65:6071–6079.

Ohtahara S, Yamatogi Y. (2006) Ohtahara syndrome: with special reference to its developmental aspects for differentiating from early myoclonic encephalopathy. *Epilepsy Res* 70(Suppl. 1):S58–S67.

Ohtahara S, Ishida T, Oka E, Yamatogi Y, Inoue H, Karita S, Ohtsuka Y. (1976) [On the specific age dependent epileptic syndrome: the early-infantile epileptic encephalopathy with suppression-burst.]. *No to Hattatsu* 8:270–279.

Piluso G, Carella M, D'Avanzo M, Santinelli R, Carrano EM, D'Avanzo A, D'Adamo AP, Gasparini P, Nigro V. (2003) Genetic heterogeneity of FG syndrome: a fourth locus (FGS4) maps to Xp11.4-p11.3 in an Italian family. *Hum Genet* 112:124–130.

Piluso G, D'Amico F, Saccone V, Bismuto E, Rotundo IL, Di Domenico M, Aurino S, Schwartz CE, Neri G, Nigro V. (2009) A missense mutation in *CASK* causes FG syndrome in an Italian family. *Am J Hum Genet* 84:162–177.

Saitsu H, Kato M, Mizuguchi T, Hamada K, Osaka H, Tohyama J, Uruno K, Kumada S, Nishiyama K, Nishimura A, Okada I, Yoshimura Y, Hirai S, Kumada T, Hayasaka K, Fukuda A, Ogata K, Matsumoto N. (2008) De novo mutations in the gene encoding STXBP1 (MUNC18-1) cause early infantile epileptic encephalopathy. *Nat Genet* 40:782–788.

Saitsu H, Kato M, Okada I, Orii KE, Higuchi T, Hoshino H, Kubota M, Arai H, Tagawa T, Kimura S, Sudo A, Miyama S, Takami Y, Watanabe T, Nishimura A, Nishiyama K, Miyake N, Wada T, Osaka H, Kondo N, Hayasaka K, Matsumoto N. (2010) *STXBP1* mutations in early infantile epileptic encephalopathy with suppression-burst pattern. *Epilepsia* 51:2397–2405.

Saitsu H, Hoshino H, Kato M, Nishiyama K, Okada I, Yoneda Y, Tsurusaki Y, Doi H, Miyake N, Kubota M, Hayasaka K, Matsumoto N. (2011) Paternal mosaicism of an *STXBP1* mutation in OS. *Clin Genet* 80:484–488.

Tarpey PS, Smith R, Pleasance E, Whibley A, Edkins S, Hardy C, O'Meara S, Latimer C, Dicks E, Menzies A, Stephens P, Blow M, Greenman C, Xue Y, Tyler-Smith C, Thompson D, Gray K, Andrews J, Barthorpe S, Buck G, Cole J, Dunmore R, Jones D, Maddison M, Mironenko T, Turner R, Turrell K, Varian J, West S, Widaa S, Wray P, Teague J, Butler A, Jenkinson A, Jia M, Richardson D, Shepherd R, Wooster R, Tejada MI, Martinez F, Carvill G, Goliath R, de Brouwer APM, van Bokhoven H, Van Esch H, Chelly J, Raynaud M, Ropers H-H, Abidi FE, Srivastava AK, Cox J, Luo Y, Mallya U, Moon J, Parnau J, Mohammed S, Tolmie JL, Shoubridge C, Corbett M, Gardner A, Haan E, Rujirabanjerd S, Shaw M, Vandeleur L, Fullston T, Easton DF, Boyle J, Partington M, Hackett A, Field M, Skinner C, Stevenson RE,

Bobrow M, Turner G, Schwartz CE, Gecz J, Raymond FL, Futreal PA, Stratton MR. (2009) A systematic, large-scale resequencing screen of X-chromosome coding exons in mental retardation. *Nat Genet* 41:535–543.

Yamatogi Y, Ohtahara S. (2002) Early-infantile epileptic encephalopathy with suppression-bursts, Ohtahara syndrome; its overview referring to our 16 cases. *Brain Dev* 24:13–23.

Zhang F, Khajavi M, Connolly AM, Towne CF, Batish SD, Lupski JR. (2009) The DNA replication FoSTeS/MMBIR mechanism can generate genomic, genic and exonic complex rearrangements in humans. *Nat Genet* 41:849–853.

Supporting Information

Additional Supporting Information may be found in the online version of this article:

Table S1. All variants identified by exome sequencing in Patient 2.

Please note: Wiley-Blackwell is not responsible for the content or functionality of any supporting information supplied by the authors. Any queries (other than missing material) should be directed to the corresponding author for the article.

Reply

Aron S. Buchman, MD,[1,2] Joshua M. Shulman, MD, PhD,[3,4] Sue E. Leurgans, PhD,[1,2] Julie A. Schneider, MD, MS,[1,2,5] and David A. Bennett, MD[1,2]

We thank Drs Jellinger and Attems for their interest in our study. In agreement with prior reports, we found that Parkinson disease (PD) pathology, including nigral neuronal loss and Lewy body pathology, is common in older adults without PD. Furthermore, we provide evidence that PD nigral pathology is related to parkinsonian motor signs in persons without a clinical diagnosis of PD.[1] This contrasts with prior studies of incidental Lewy body disease, which found associations with subtle electrophysiologic changes but not with overt motor signs.[2] Interestingly, in the current study, we also found that Alzheimer disease (AD) and cerebrovascular pathology showed independent associations with the severity of parkinsonian motor signs.[1] As requested, the correlations among these common brain pathologies are included in the accompanying Table. It is interesting that Dr Attems and colleagues did not find an association of nigral pathology or cerebrovascular disease with parkinsonian signs among persons with AD.[3] We and others have reported such associations.[4–6] Overall, the findings in the current study have important public health implications. They suggest that mild parkinsonian signs, reported in up to 50% of older adults by age 85 years and associated with significant morbidity and mortality, may be caused by a range of pathologies including PD pathology, AD, and cerebrovascular pathologies. These data underscore the need for more sensitive clinical measures and biomarkers that can detect and differentiate the various neuropathologies underlying the development of parkinsonian signs in old age.

Potential Conflicts of Interest

Nothing to report.

[1]Rush Alzheimer's Disease Center and [2]Department of Neurological Sciences, Rush University Medical Center, Chicago, IL, [3]Department of Neurology, Brigham and Women's Hospital, Boston, MA, [4]Department of Neurology, Harvard Medical School, Boston, MA, and [5]Department of Pathology (Neuropathology), Rush University Medical Center, Chicago, IL

References

1. Buchman AS, Shulman JM, Nag S, et al. Nigral pathology and parkinsonian signs in elders without Parkinson disease. Ann Neurol 2012;71:258–266.
2. Caviness JN. Presymptomatic Parkinson's disease: the Arizona experience. Parkinsonism Relat Disord 2012;18(suppl 1):S203–S206.
3. Attems J, Quass M, Jellinger K. Tau and α-synuclein brainstem pathology in Alzheimer disease: relation with extrapyramidal signs. Acta Neuropathol 2007;113:53–62.
4. Burns JM, Galvin JE, Roe CM, et al. The pathology of the substantia nigra in Alzheimer disease with extrapyramidal signs. Neurology 2005;64:1397–1403.
5. Schneider JA, Li JL, Li Y, et al. Substantia nigra tangles are related to gait impairment in older persons. Ann Neurol 2006;59:166–173.
6. Buchman AS, Leurgans SE, Nag S, et al. Cerebrovascular disease pathology and parkinsonian signs in old age. Stroke 2011;42:3183–3189.

DOI: 10.1002/ana.23639

Whole Exome Sequencing Identifies *KCNQ2* Mutations in Ohtahara Syndrome

Hirotomo Saitsu, MD, PhD,[1] Mitsuhiro Kato, MD, PhD,[2] Ayaka Koide, MD, PhD,[3] Tomohide Goto, MD, PhD,[3] Takako Fujita, MD,[4] Kiyomi Nishiyama, PhD,[1] Yoshinori Tsurusaki, PhD,[1] Hiroshi Doi, MD, PhD,[1] Noriko Miyake, MD, PhD,[1] Kiyoshi Hayasaka, MD, PhD,[2] and Naomichi Matsumoto, MD, PhD[1]

Recently, Weckhuysen et al revealed that *KCNQ2* mutations are involved in a substantial proportion of patients with a neonatal epileptic encephalopathy.[1] Some cases showed a suppression–burst pattern on electroencephalogram (EEG), tonic seizures, and profound intellectual disability, resembling Ohtahara syndrome (OS). By whole exome sequencing analysis of 12

TABLE: Intercorrelation of Postmortem Indices

Index	Macroinfarcts	Microinfarcts	Arteriolosclerosis	AD Pathology	Nigral Lewy Bodies
Nigral neuronal loss	0.07, 0.068	0.02, 0.628	0.13, <0.001	0.14, <0.001	0.38, <0.001
Macroinfarcts	—	0.39, 0.056	0.26, <0.001	0.09, 0.017	−0.063, 0.072
Microinfarcts		—	0.15, <0.001	0.04, 0.315	−0.10, 0.075
Arteriolosclerosis			—	0.03, 0.385	0.03, 0.491
AD pathology				—	0.07, 0.052

Based on Spearman or tetrachoric correlation and *p* value.